REPORT DOCUMENTATION PAGE

Form Approved
OMB No. 0704-0188

PLEASE DO NOT RETURN YOUR FORM TO THE ABOVE ORGANIZATION.

1. REPORT DATE *(DD-MM-YYYY)*	2. REPORT TYPE	3. DATES COVERED *(From - To)*
	FINAL REPORT	15 Apr 2004 - 14 Oct 2006

4. TITLE AND SUBTITLE
(QC THEME) RESONANT QUANTUM DEVICE TECHNOLOGIES

5a. CONTRACT NUMBER

5b. GRANT NUMBER
FA9550-[redacted]0-04-1-0285

5c. PROGRAM ELEMENT NUMBER
61102F

6. AUTHOR(S)
PROFESSOR FAINMAN

5d. PROJECT NUMBER
2304/SX

5e. TASK NUMBER

5f. WORK UNIT NUMBER

7. PERFORMING ORGANIZATION NAME(S) AND ADDRESS(ES)
UNIVERSITY OF CALIFORNIA
9500 GILMAN DRIVE 0934
LA JOLLA CA 92093-0934

8. PERFORMING ORGANIZATION REPORT NUMBER

9. SPONSORING/MONITORING AGENCY NAME(S) AND ADDRESS(ES)
AF OFFICE OF SCIENTIFIC RESEARCH
875 NORTH RANDOLPH STREET ROOM 3112
ARLINGTON VA 22203
DR GERNOT POMRENKE/NE

10. SPONSOR/MONITOR'S ACRONYM(S)

11. SPONSOR/MONITOR'S REPORT NUMBER(S)

12. DISTRIBUTION/AVAILABILITY STATEMENT
DISTRIBUTION STATEMENT A: UNLIMITED

AFRL-SR-AR-TR-07-0228

13. SUPPLEMENTARY NOTES

14. ABSTRACT

From 2005-2006 success was made in incorporating the nanocrystal into Polymethl methacrylate (PMMA) matrix. The sensitivity of this composite to electron beams makes it attractive in the fabrication of photonic devices. From 2004-2005, numerical simulations were made for experimentally plausible system parameters for the network sending a single photon wavepacket and for entanglement between two nodes. The team continued optimizing the properties of the quantum dot composites and succeeded to make the nanocomposites in both PMMA and SU-8 hosts with high level of uniformity. A near field optical characterization tool for nanophotonic devices was developed. A study was started on excitation of ultrashort pulse surface plasmon polariton (SPP) fields as well as an investigation of ultrafast electrodynamics of the ultrashort SPP wavepackets. From 2003-2004 the team completed a theoretical study on nonlinear phase shift in the system with a quantum dot embedded in a two-sided cavity from the weak-coupling regime to the strong coupling regime. Additionally, the team developed an approach to manufacture photonic

15. SUBJECT TERMS

crystal-based on a two-step process consisting of holographic lithography patterning to define the photonic crystal lattice followed by optical direct-write of the functional elements.

16. SECURITY CLASSIFICATION OF:			17. LIMITATION OF ABSTRACT	18. NUMBER OF PAGES	19a. NAME OF RESPONSIBLE PERSON
a. REPORT	b. ABSTRACT	c. THIS PAGE			19b. TELEPHONE NUMBER *(Include area code)*

UNIVERSITY OF CALIFORNIA, SAN DIEGO

BERKELEY • DAVIS • IRVINE • LOS ANGELES • RIVERSIDE • SAN DIEGO • SAN FRANCISCO

SANTA BARBARA • SANTA CRUZ

DEPARTMENT OF ELECTRICAL AND COMPUTER ENGINEERING
9500 GILMAN DRIVE
LA JOLLA, CALIFORNIA 92093-0407

Y. Fainman
858-534-8909
fainman@ece.ucsd.edu

March 23, 2007

Dr. Gernot S. Pomrenke, PhD
Program Manager - Optoelectronics and Nanotechnology
AFOSR/NE
Directorate of Physics and Electronics
Air Force Office of Scientific Research
Ballston Common Towers II
801 N. Randolph Street, Room 732
Arlington VA 22203-1977
e-mail: gernot.pomrenke@afosr.af.mil
Tel: 703-696-8426
Fax: 703-696-8481

Dear Dr. Pomrenke:

Please find enclosed the Final report for the grant FA9550-04-1-0285 entitled "Resonant Quantum Device Technologies," by Y. Fainman, L. J. Sham, and C. W. Tu , at UCSD.

Should you have any questions about this report, please do not hesitate to contact me.

Sincerely,

Y. Fainman
Professor

Annual Technical Report

for AFOSR

Resonant Quantum Device Technologies

Sponsored by

Air Force Office of Scientific Research

Under Grant FA9550-04-10285

for Period 4/15/04 through 10/14/06

total: $589,328

Grantee

The Regents of the University of California, San Diego

University of California, San Diego

La Jolla, CA 92093

Principal Investigators: Y. Fainman (UCSD), (858) 534-8909

co-Principal Investigators: L. J. Sham (UCSD), C. W. Tu (UCSD)

Program Manager: Dr. G. Pomrenke, (703) 696-8426

2. Objectives/Statement of work

1. *Theoretical Analysis and Design of Resonant Quantum Devices:* The theoretical effort is focused on design and simulation of the optoelectronic devices for information processing of a mixture of quantum and classical information with special emphasis on nanophotonic devices.
2. *Fabrication of Quantum Devices*: The fabrication effort is focused on developing nanofabrication techniques for resonant quantum devices including growth of III-V based quantum dots and cavities for operation at the telecommunication wavelength, advanced holographic lithography to achieve large area photonic crystal lattice that can be used to define photonic device elements and circuits, and integration of colloidal quantum dots based on II-VI and IV-VI compound semiconductors into polymer that can be patterned to fabricate quantum devices. We also explore surface plasmon-polariton phenomena that holds great potential for confinement of optical fields which is essential to enhance linear and nonlinear interactions with quantum systems such as semiconductor quantum dots.
3. *Characterization of nanophotonic quantum devices:* The characterization of nanophotonic devices effort will focus on developing novel nonlinear optical characterization tools at cryogenic temperatures and near field optical microscope with the goal to operate it with nanoscale spatial and femtosecond scale temporal resolution. Additionally, for operation and control of quantum devices we need to devise ulra high resolution optical waveforms synthesis methods that can be optimized for coherent control of quantum systems that are being investigated and operated on time scales of 10-100 psec..

4. Status of effort

Period 2003-2004:

1. In order to assess the capability of a quantum dot (QD) cavity system as a compact replacement for the nonlinear Kerr medium for optical quantum information processing, we completed a theoretical study on nonlinear phase shift in the system with a QD embedded in a two-side cavity from the weak-coupling regime to the strong-coupling regime [1]. Fig.1 shows the phase shift for a coherent pulse light which contains one photon on average for an InAs dot as a function cavity Q factor and the exciton-cavity coupling g. The value of g=0.1 meV is now achieved by our collaboration team [Scherer Nature article]. For equivalent phase shift, the length of the Kerr medium with the best nonlinearity would be of the order of one meter.

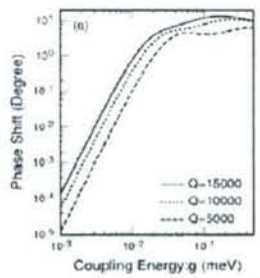

Fig. 1. Nonlinear phase shift in a cavity containing QD as a function of g and Q

2. We have shown how a fundamental node (Fig. 2) can be built with a coupled system of a quantum dot,

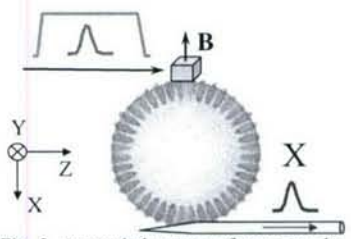

Fig. 2. A coupled system of quantum dot, cavity and wave guide, illustrating how optical pulse control can lead to emission of a single photon wave packet.

cavity and wave guide, based on our theory of the quantum electrodynamics of the excited state (trion) of a spin qubit in the dot interacting with the cavity photon which is coupled to the photon wavepacket in the wave guide. The optical process involves laser control of the trion of the dot and the output or input of the wavepacket via the wave guide. The node and wave guide may be formed into a quantum net [3], or be used for distributed quantum computing [4], or used to enhance photon-photon interaction such as in a phase gate [2].

3. We have developed an approach to manufacture photonic crystal-based devices based on a two-step process consisting of holographic lithography patterning to define the photonic crystal lattice followed by optical direct-write of the functional elements. First, the photonic crystal lattice is patterned in photoresist using holographic optical lithography with multiple exposures, producing a large-area (about 1 cm^2) lithographic pattern quickly and easily (Fig. 2a). In the second step, the variations or defects in the lattice to implement the functional devices are created using optical direct-write with a strongly focused optical beam (see Fig. 2b). After the patterning processes, the mask is developed and a dry-etching process (with the CAIBE system) is used to transfer the desired pattern into a high dielectric constant GaAs substrate (Fig. 2c). With optimized dry-etching parameters, a vertical sidewall etched profile was achieved. The erosion rate of the resist and the etching rate of GaAs are 5 nm/min and 16 nm/min, respectively, such that the etching rate selectivity is approximately 3:1. Since the entire large-scale photonic crystal lattice is essentially created at once using interferometric patterning (Fig. 2a), the direct-write process is needed only to implement the functional elements (e.g., waveguides in Fig. 2b, cavities, etc.) instead of the entire lattice. The negative photoresist nature of SU-8 allows for further modification of the exposed photonic crystal lattice by selective point-by-point exposure of areas that have not yet been exposed. Such a process may be used to introduce point defects to create 2-D nanocavity, line defects to create a linear waveguide as well as any desired pattern in principle. To achieve high resolution for direct-write the line defect, we choose a reflective microscope objective lens 36X (0.52NA) with focal length of 10.4mm (from Thermo Oriel). We used vertical axis of

(a) (b) (c) (d)

Fig. 2. Fabrication of large area photonic crystal lattice and photonic circuits: (a) Hexagonal structure lattice in resist is exposed to create a (b) 2-D photonic hexagonal photonic crystal in resist with waveguide; using CAIBE the resist mask is transferred into GaAs substrate (c) photonic crystal and (d) photonic crystal with a waveguide

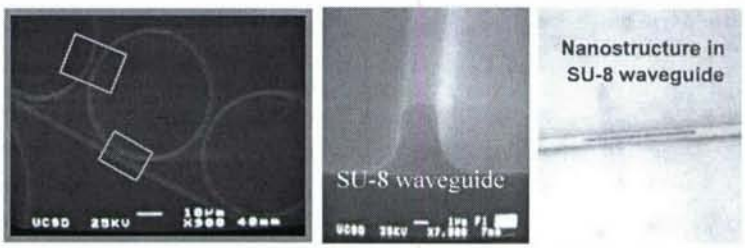

Fig. 3 Ring cavities coupled to waveguide fabricated in polymer.

our optical table to achieve high precision alignment by aligning the axis of the interference pattern to the translation stage axis in the translation direction. Thus, this hybrid approach possesses an advantage in terms of fabrication time and cost as compared to E-beam lithography for the patterning of large-scale photonic crystal-based integrated systems. We have also started to make resonant ring cavities and coupled ring cavities (see Fig. 3) and will explore using this geometries for realization of quantum phase gates using colloidal quantum dots integrated into polymer or SU-8 nanocomposites.

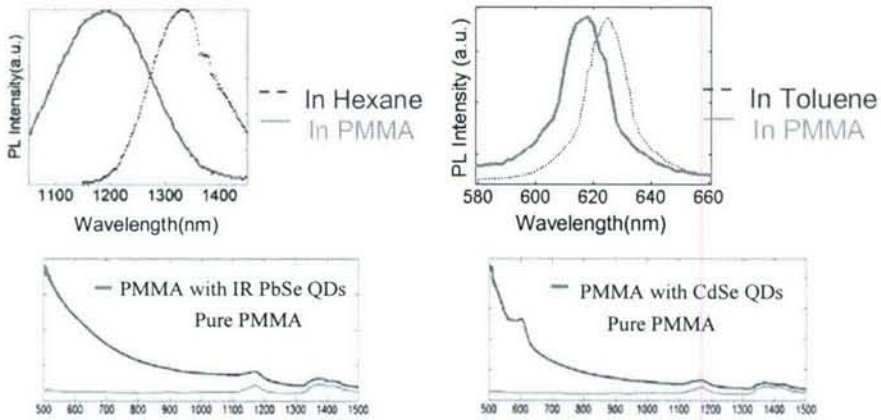

Fig. 4. Photolumenescence and absorption spectra of PbSe and CdSe quantum dots-PMMA nanocpomposites.

4. We continued developing fabrication process of quantum dot composites and sucseeded to make the nanocomposites in both PMMA and SU-8 hosts. The process uses commercially available colloidal II-VI and IV-VI quantum dots and mixes them into resist for patterning to create photonic devices and circuits . This method allows us to construct photonic devices. To avoid cluster aggregation within the bulk polymer matrix in contrast to previous approaches based on using ligand and other surfactants we suspended QDs in the MMA during polymerization step. When MMA polymerizes to PMMA, the large molecular weight PMMA with enveloped QDs sinks to the bottom of the container, whereas the non-polymerized MMA moves towards the top. Furthermore, due to the higher solubility of QDs in non-polymerized MMA, the non-wrapped QDs diffuse to the top MMA layer, leaving a gap in the middle region. We resolved this issue using pre-polymerization method: The MMA QDs solution was heated in a thermostatic water bath at about 90°C for 20 min to obtain the desired viscosity, or pre-polymerization, and then poured into molds, which were heated at 60°C for ~ 20h to achieve post-polymerization. We optimized synthesis of composite

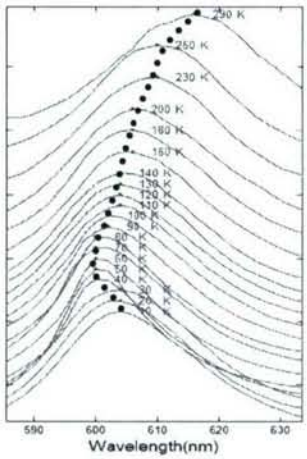

Fig. 5 Dependence of the PL spectrum on the temperature for quantum dot nanocomposites in PMMA

semiconductor quantum dots into resist, varying the optical photoluminescence range, density of dots as well and structure of the pattern applied to these resists: different dots and at different concentrations. The nanocomposites have been characterized by measuring the PL for both PbSe and CdSe quantum dots nanocomposites in PMMA (see Fig. 4). Low temperature measurements show blue shift of the quantum dots in PMMA of about 16 nm (see Fig. 5).

5. We also initiated fabrication of nano- and microstructures using the nanocomposite quantum dots in PMMA and SU-8. For PMMA nanocomposite we used standard E-beam lithography method. An SEM of a periodic nanostructure with features of 200-300 nm made out of such a resist is shown in Fig. 6. We have also started to fabricate photonic resonant structures from SU-8 nanocomposites utilizing the uniqueness of negative resist that we need just to expose the regions of the desired devices. We fabricated coupled rings configurations as they are essential for realization of quantum phase gate as designed in 1 and 2 (see Fig. 7a). We also fabricated a spiral structure to achive a compact package for a very long

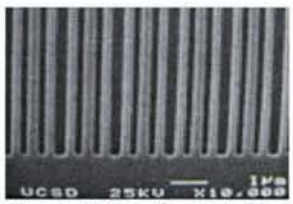

Fig. 6. SEM of a periodic structure in a quantum dot composite resist.

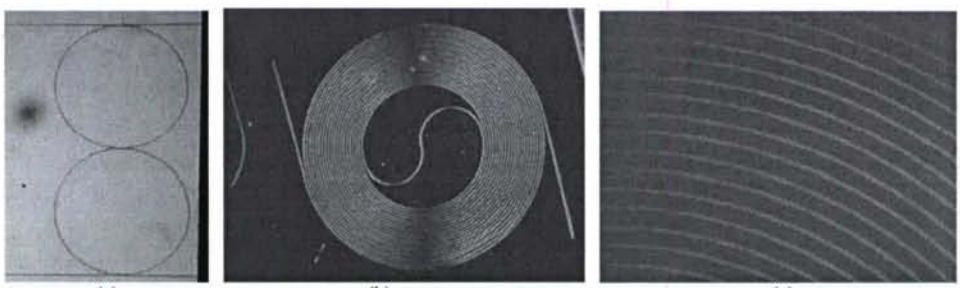

(a) (b) (c)

Fig. 7. Structures fabricated in SU-8 nanocomposites. (a) coupled ring cavity for implementation of phase gate, (b) a spiral shape waveguide under UV illumination, (c) enlarged part of (b).

This configuration may be possible to use for realization of a compact quantum dots based amplifier. UV illuminated structure is shown in Fig. 7b and enlarged portion in Fig. 7c.

6. We continued construction of a unique all-fiber near-field optical microscope for measurement of the complex amplitude of the near field on the nanoscale at operating wavelengths around 1.55 μm, extending

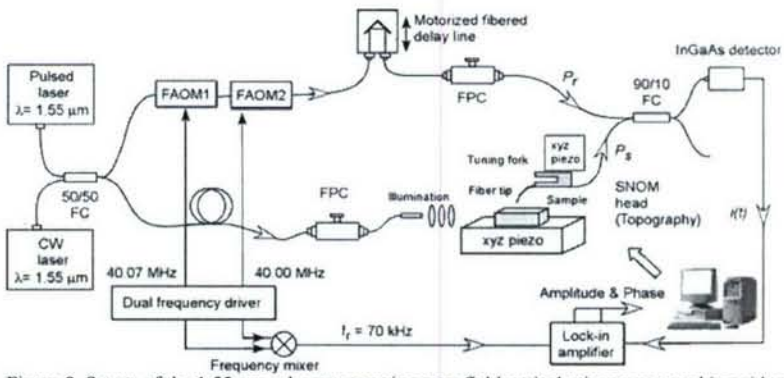

Figure 8. Set-up of the 1.55 um coherent scanning near-field optical microscope working either with CW or ultra-short pulses.

its design and operation with femtosecond laser pulses and in a broad spectral range for investigation of both linear and non linear optical phenomena in the near field. The coherent NSOM is implemented with a combination of an NSOM and an interferometer (heterodyne in our case). We use an all fiber-based system design to achieve interferometric stability and operate the system at a telecommunication wavelength in the infrared range (~1.55 μm) to meet the need in building characterization tools for better understanding nanophotonic devices for telecommunication applications. Also, our interferometric detection system can work either with CW light or ultrashort pulses. For the pulsed system, an optical delay line is used for temporal pulse correlation with τ=2 fs resolution steps. A schematic diagram of the set-up is presented in Fig. 8. The 1.55 μm laser is split to create a reference with a frequency shifted using two acousto-optic modulators. The second beam is used for illumination in different configurations, according to the desired measurement (collection mode, illumination mode, waveguide injection collection mode). The polarization mode is adjusted using a fiber polarization controllers. A fiber tip is brought close to the surface using an atomic force microscope (AFM). The NSOM tip is mounted on a tuning fork and an electronic feedback controls the sample-tip distance within a few nanometers. The commercial AFM (Nanonics TS-2000) is composed of two flat piezoelectric scanners permitting either the tip or the sample to be moved. The light (propagating or evanescent) emerging from the structure is collected by the fiber tip. The signal and the reference beams are recombined into an InGaAs detector for post signal processing and analysis. For the functional characterization on nanophotonic devices we use a waveguide implemented in a photonic crystal lattice. The PC waveguide, consisting of a missing row of holes in a square-lattice PC structure, is shown in Fig. 9. The experimental measurements are performed using a heterodyne SNOM system designed to operate at wavelengths around 1.55 μm. A solid-state laser with a tunable range of 1520–1580 nm is used as the light source. The detected amplitude and phase for light of wavelength 1560 nm propagating in the PC waveguide are shown in Figs. 10a and 10b, respectively. The amplitude image clearly shows that the light is mostly confined to the waveguide channel. Looking also at the phase image, we observe that most of the guided light appears to be propagating in a single mode having even transverse symmetry. Furthermore, Fig. 10b shows a distinct phase pattern having transverse phase fronts in the region of the waveguide channel, with a period

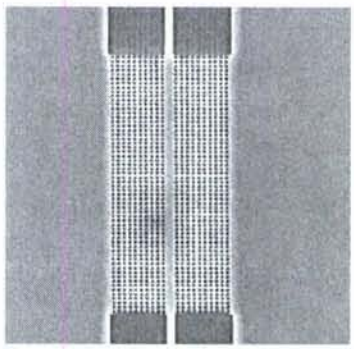

Fig. 9. SEM picture of the photonic crystal waveguide, consisting of a missing row of holes in a Silicon square-lattice photonic crystal membrane and a tapered ridge waveguide for light injection. The waveguide length in the membrane is 30 μm, and the lattice period is 496 nm.

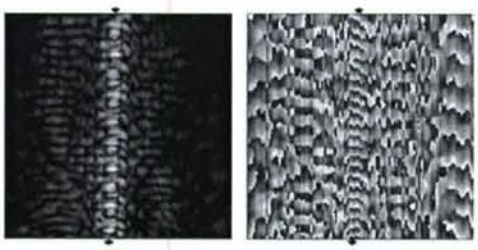

(a) (b)

Fig. 10 Observed (a) amplitude and (b) phase over a 14 μm square area for 1560nm light propagating in a square-lattice photonic crystal waveguide detected using heterodyne SNOM. The diamond symbols at the edges of the images indicate the approximate position of the

significantly smaller than in the surrounding area as expected. In addition, we also investigate the spectral characteristics of light guided in this structure. The amplitude and phase images taken with the heterodyne SNOM for light at three different wavelengths are shown in Fig. 11. At a vacuum wavelength of 1541 nm (Figs. 11a and 11b) we observe a change in the mode. In this case, most of the light propagates in an odd mode having transverse maxima at the edges of the waveguide channel. This suggests that different modes are dominant at these two wavelengths. At a wavelength of 1533 nm (Figs. 11c and 11d), the light appears to still be guided, although significantly more scattering is observed. At a wavelength of 1521 nm (Figs. 11e and 11f), a significant amount of light escaping the waveguide channel can be seen. In summary, we have demonstrated the direct observation of the amplitude and phase of an optical field propagating inside a PC waveguide using heterodyne SNOM. In addition, we have observed a change in the propagating mode in the waveguide corresponding to changes in the optical wavelength, and found an agreement between near-field and far-field measurements. Further comparisons of experimental measurement results with theoretical predictions could provide further insight into the design and optimization of PC waveguides and other nanostructured devices. Finally, application of this technique to the study of other subwavelength-scale photonic devices could advance the understanding of light propagation phenomena in a variety of nanostructured devices and systems

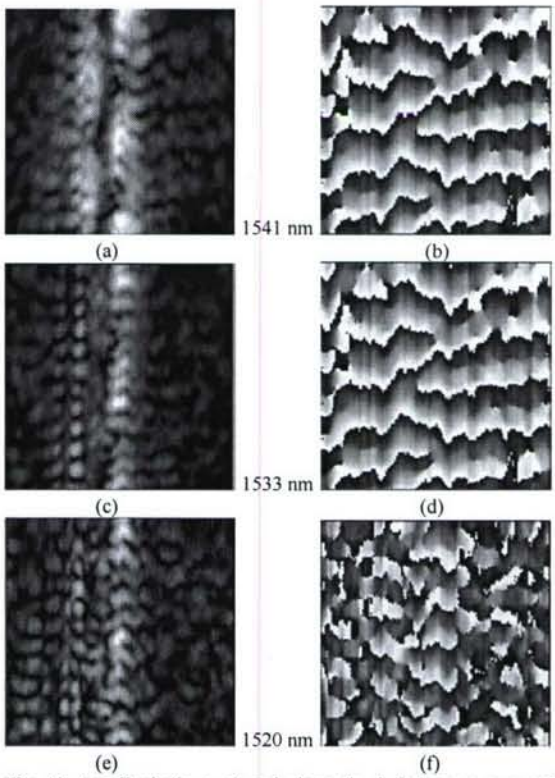

Fig. 11. Amplitude (a, c, e) and phase (b, d, f) images over a 7 μm square area taken with the heterodyne SNOM of light propagating in the PC waveguide at various wavelengths: (a,b) 1541 nm; (c,d) 1533 nm; (e,f) 1520 nm.

Period 2004-2005:

1. At the heart of this proposed solid state system for quantum network and distributed computation is a scheme of quantum control for arbitrary interchange between a stationary qubit and a flying qubit (carried by single photon wavepacket) at a quantum interface composed of a single quantum dot containing either two excitons or a spin coupled to a photon continuum through a resonant cavity. It can be used for generation or reception of an arbitrarily shaped single-photon wavepacket. The generation process can also be controlled to create entanglement between stationary qubit and flying qubit. The generation and reception operation can be combined to perform quantum network operations such as transfer, swap or entanglement creation of qubits between distant nodes. Numerical simulations were made for experimentally plausible system parameters for the network sending a single photon wavepacket and for entanglement between two nodes.

2. We continued optimizing the properties of the quantum dot composites and sucseeded to make the nanocomposites in both PMMA and SU-8 hosts with high level of uniformity. We also focused our effort to reduce the concentration of semiconductor quantum dots in PMMA and create ultrathin samples such that we can easily fing single quantum dots using conventional microscopes. These samples are being used in spectroscopic measurements at few degrees K. Our preliminary experimental results show both biexitonic and oscillatory behaviour. We are in the process of analyzing and interpreting these experimental data and correlating it with theory.

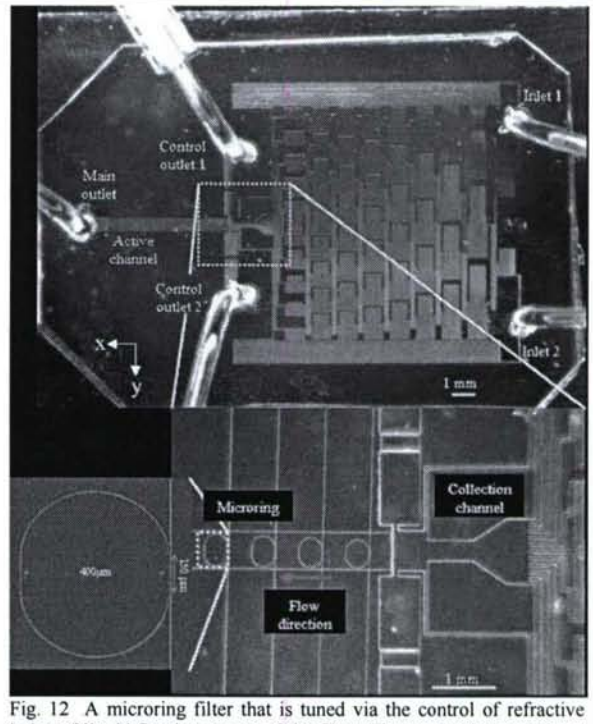

Fig. 12 A microring filter that is tuned via the control of refractive index of liquid flowing on top of the filter. The top section contains a microfluidic chip allowing on-chip mixing of 2 liquids with different refractive index. The mixer creates a linear index profile along the y-axis in the collection channel. By controlling the pressure difference between the two control outlets a narrow portion of the index profile is selected to flow into the "active" channel. The evanescent tail of the waveguide mode in the microring overlaps with the liquid cladding, thereby tuning the effective refractive index of the microring and the coupling coefficient between the ring and bus waveguides.

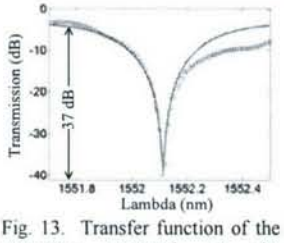

Fig. 13. Transfer function of the resonator operated at the optimized value of the cladding to achieve critical coupling

3. The fabrication of resonant structures at a specific precisely defined resonance frequency that matches that of a quantum dot resonance has been a challenging tast primarily due to the fabrication tolerances. We developed a new method that allows to overcome this issue. Our approach uses a fluidic cladding over the resonant structures where the refractive index of the fluid can be very accurately tuned to reach the desired resonance. Specifically we constructed a microfluidic mixer integrated with resonant ring microcavities shown in Fig. 12. The experimental characterization of our device shows extinction ratio of 37 dB. In comparison with currently reported performance of under 15 dB, our devices shows significant performance enhancement of over 20dB.

4. We also continued developing our near field optical characterization tool for characterization of near field optical nanophotonic devices. Specifically we demonstrated for the first time the existence of two types of modes in a photonic crystal waveguide. A band diagram of our fabricated photonic crystal lattice waveguide is shown in Fig. 14. There are two wavegide modes e1 and e2 which are excited at different optical frequencies. e1 lies abow the free space line and therefore is more lossy (leaky mode) whereas the e2 mode is propagating mode. Fig. 15 shows The redistribution of amplitude in the two modes. However, most important results of our measurement is

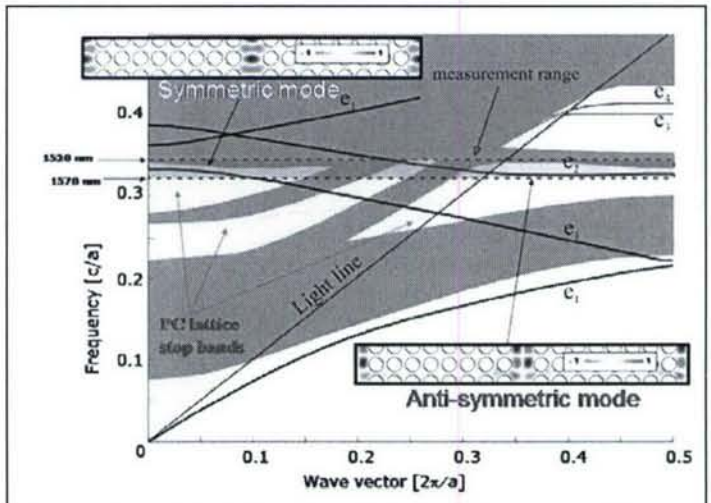

Fig. 14. Band structure of a photonic crystal lattice with a one row defects implementing a photonic crystal waveguide.

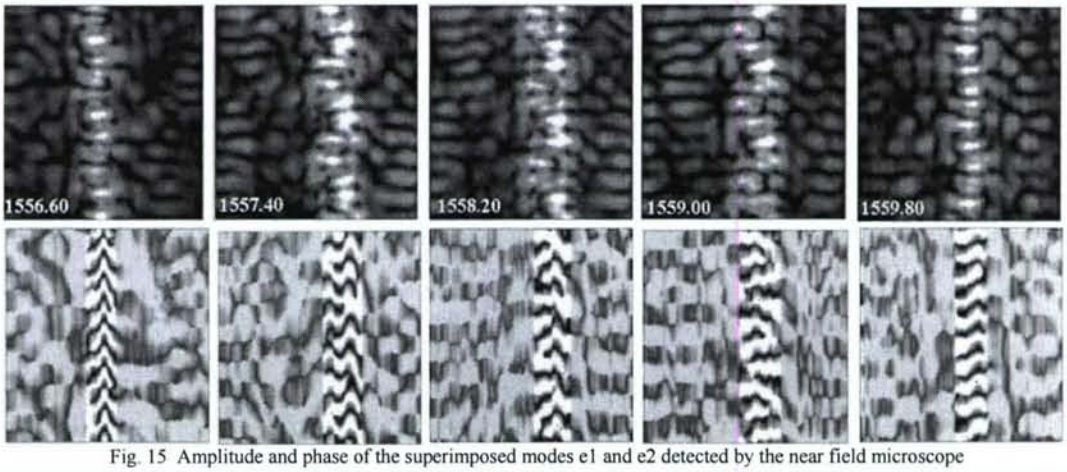

Fig. 15 Amplitude and phase of the superimposed modes e1 and e2 detected by the near field microscope

both amplitude and phase of the modal structures propagating in the photonic crystal waveguide. Using the complex amplitude of the detected field we performed a Fourier Transform in the propagation ditection of the field and found the bpropagation constants β for the 2 modes as evident from the Fig. 16.

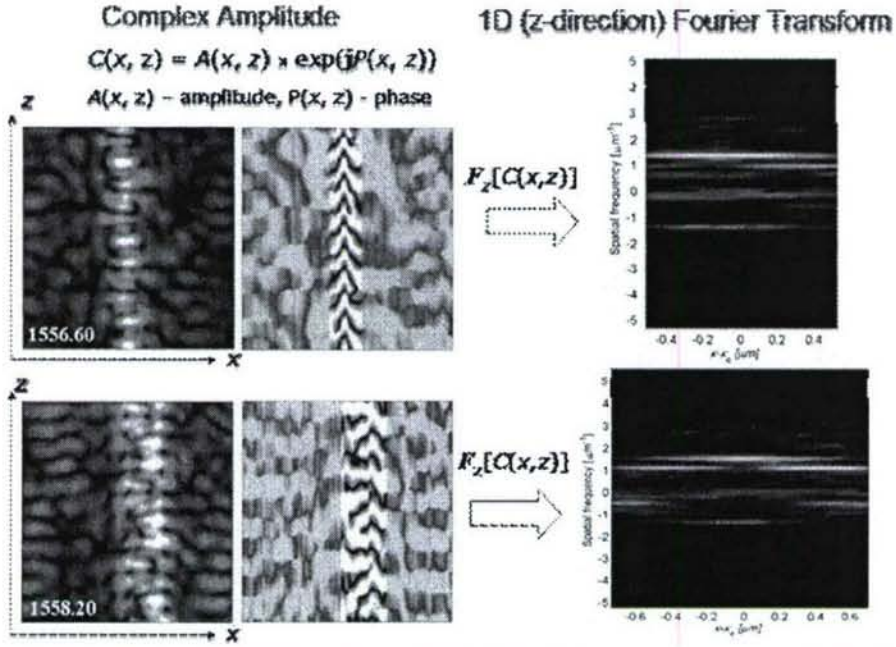

Fig. 16 Spectrum of the near field complex amplitude showing spatial frequency content of the excited mode structure as a function of the excitation frequency

5. We recently started a study on excitation of ultrashort pulse surface plasmon polariton (SPP) fields and investigated ultrafast electrodynamics of these ultrashort SPP wavepackets. For the excitation and visualization of propagation of ultrashort SPPs we fabricated a number in samples of nanohole arrays on a total area of 200x200 micrometers.

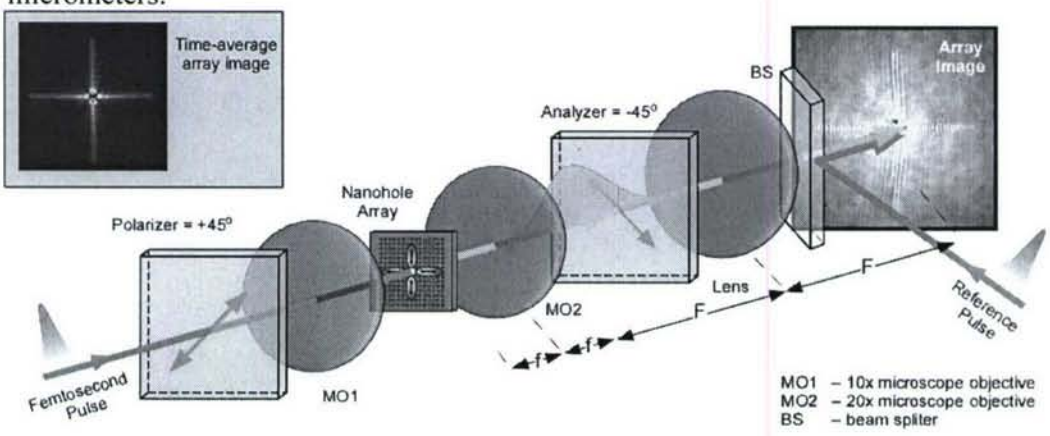

Fig. 17 Experimental apparatus for excitation and visualization of ultrashort SPPs

The samples were fabricated using such metals as gold. silver, and aluminum on various substrates such as glass, alumina, GaAs, and Si. We have excited SPP on a single side of Metal-Dielectric boundary as well as on both sides depending on the thickness of the metal which was varied from 20-100nm. The experimental apparatus is shown schematically in Fig. 17. We used image heterodyne detection method followed by signal processing that allows us to detect amplitude and phase of the ultrashort pulse SPP. Snap shoots of ultrashort pulse SPP propagating and scattered from the nanohole array is shown in Fig. 18.

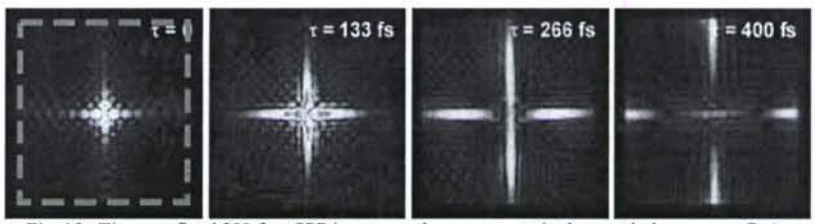

Fig. 18. Time confined 200 fsec SPP images as they propagate in the nanohole array on GaAs

We also investigated transfer of optical phase onto the ultrashort pulse SPP wavefront in order to investigate SPP focusing properties. This results reveal that we can transfer optical phase onto the SPP phase and thereby manipulate plasmonic fields from the optical fields. The results of this study are summarized in Fig. 19.

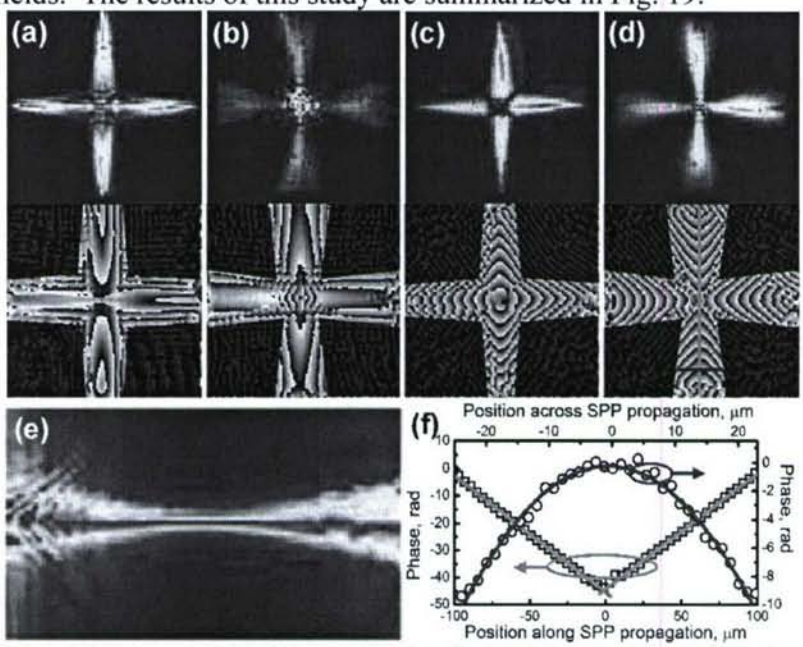

Fig. 19. Spatial evolution of scattered SPP field. (**a-d**) Spatial amplitude and phase (modulo 2p) distributions of scattered SPP pulse measured with 1.6 mm (a, b) and 1.4 mm (c, d) nanohole array periods with converging (a, c) and diverging (b, d) Gaussian beam illumination showing SPP field focusing and defocusing within metallic film surface. Red and blue lines in phase distribution (d) show direction of cross-sections for phase plots in (f). Spatial phase distributions demonstrate direct (a, b) and inverse (c, d) phase relationship between incident optical field and scattered SPP field. (**e**) in-plane SPP focal waist formation, measured in nanohole array with 1.6 mm period. Amplitude is renormalized in SPP propagation direction (horizontal) to compensate for attenuation. (**f**) unwrapped longitudinal (open squares) and transversal (open circles) cross-sections of the spatial phase distribution from (d) with linear and quadratic least-squares fitting plots. Linear phase corresponds to 6.0 degrees phase matching angle for (-1,0) and (0,-1) SPP modes., while quadratic spatial phase of SPP field in is acquired from the quadratic spatial phase of the incident optical field.

6. For operation and control of quantum devices we need to devise ulra high resolution optical waveforms synthesis methods that can be optimized for coherent control of quantum systems that are being investigated and operated on time scales of 10-100 psec.

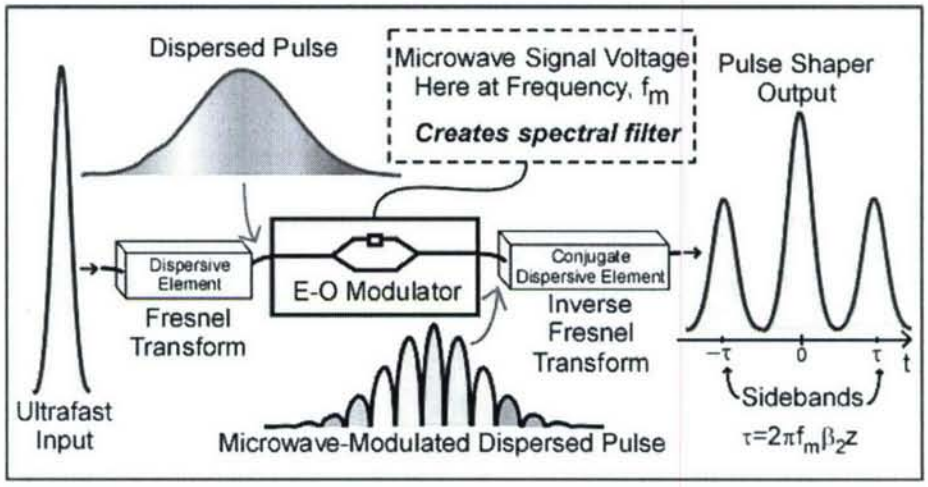

Fig. 20 Longitudinal ultra-high resolution waveform synthesizer for coherent control of quantum devices and systems

Our approach, shown schematically in Fig. 20 is based on longitudinal spectral decomposition. In contrast to existing approaches that use transverse spectral decomposition, our method allows to achieve time bandwidth product of 10,000-100,000, which is about 100 better than what can be achieved with compact pulse shapers implemented in free space using transverse spectral decomposition. Our implementation uses conjugate dispersive components (single mode fiber and dispersion compensated fiber as well as a matched pair of chirped fiber Bragg gratings) in combination with fast electro-optic modulators. The method has been used for experimental validation showing expected performance. For example when the modulator is used for single tome RF modulation with a bias to suppress the carrier, we observed 3 pulses in the autocorrelation trace as expected for such synthesized waveform (see Fig. 21).

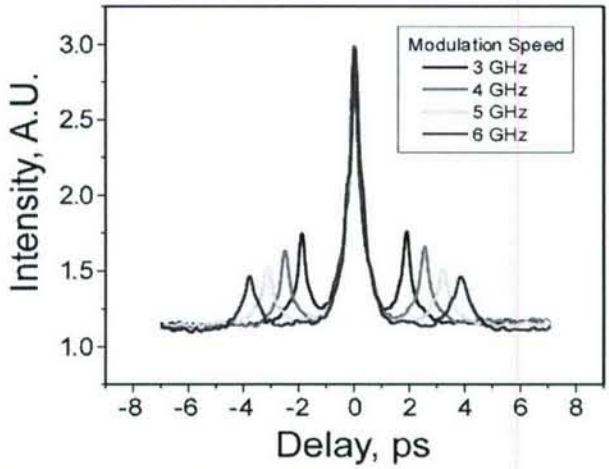

Fig. 21. An autocorrelation trace of a synthesized ultrafast waveform for various settings of the RF signal applied to the electro-opticv modulator in the waveform synthesized based on longitudinal spectral decomposition.

Period 2005-2006:

1. We continued the study of semiconductor quantum dots (QDs) formed in colloidal solution, called nanocrystal (NC), via chemical synthesis. In colloidal solutions, however, NC's are suspended in a solvent, making them less practical for fabrication and integration of photonic and optoelectronic devices. The introduction of such NC's into a solid-state matrix, therefore, is of great interest for numerous applications. We have succeeded in incorporating the NCs into Polymethyl methacrylate(PMMA) matrix (as described above). The sensitivity of this composite to electron beams makes it attractive in the fabrication of photonic devices. We particularly studied the spectra of single NC in PMMA. It's useful for the future application of single NC in PMMA photonics device. Our study is primarily focused on the quantum information applications.

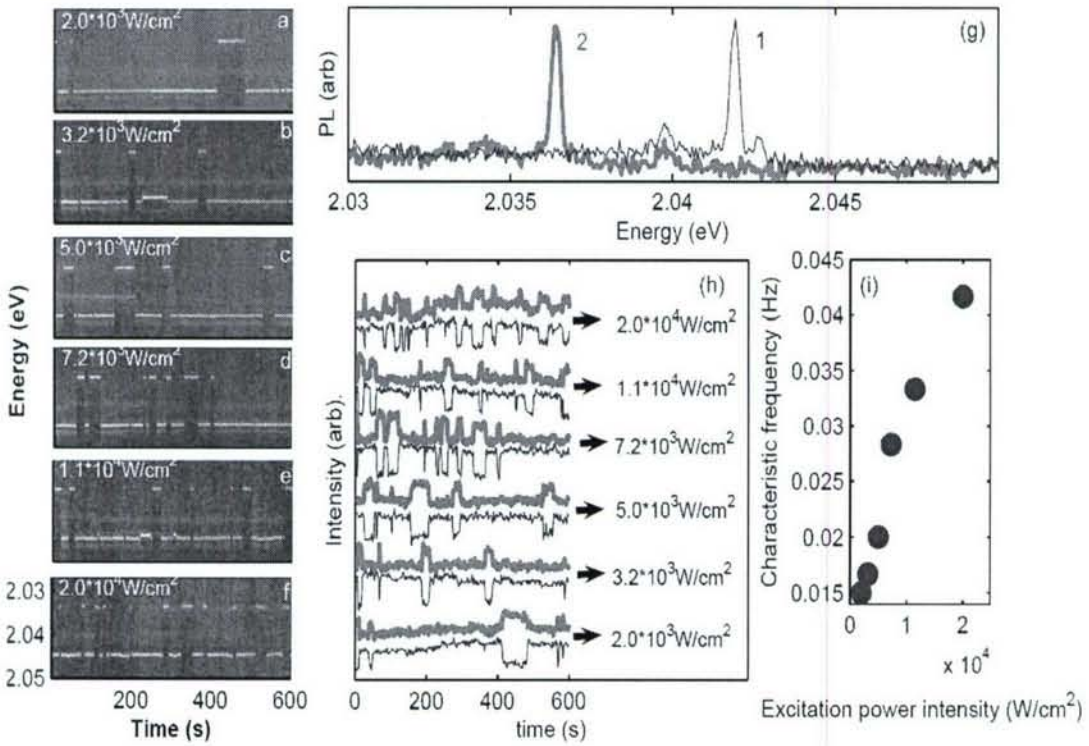

Fig. 22. Spectra from a typical switching NC's, recorded at six different excitation powers (2.0,3.2,5.0,7.2,11,20*103W/cm2) are shown in order in (a)-(f). The integration time 2 s is used for this measurement. The brightness represents the intensity, the horizontal axis is the time and the vertical axis is emission energy. (g) is the integration for 26 measurements (each measurement has 2 s integration time) when the NC's stay in the same state. The energy difference between the two states is 5.6 meV. (h) intensity vs. time plot for Fig.1(a)-1(f). The (blue) thin line is for the high energy state. (i) The characteristic switching frequency vs excitation power.

We conducted a series of experiment on spectroscopy of NC in PMMA at cryogenic temperatures in order to better understand their quantum coherence properties and effects. Specifically, we found and investigated several quantum dots switching between two states. Spectra from a typical switching NC, recorded at six different excitation powers, are shown in

Fig. 22 (a)-(f).These spectra are recorded continuously with an integration time of 2 s each. The greyscale plot represents intensity, while the horizontal axis is time, and the vertical axis is the emission energy. Fig. 22(g) shows the typical spectrum for the two states. The red line (bold line) is for the lower energy state, which we will call state 2, while the blue line (thin line) is for the higher energy state which we call state 1. The energy difference between the two states is 5.6 meV. Fig. 22(h) is a plot of intensity vs. time for data taken from Fig. 22(a)-(f). Fig. 22(i) is the plot of the characteristic frequency vs excitation. power. From Fig. 22(g) and 22(h) we see that there is no sizable change in the integrated PL intensity for the two states. The excitation power density is of the order of 10 kW/cm^2. Figure 22 shows that state 1 dominates at low excitation powers while state 2 is more pronounced at high excitation powers. In addition, the switching frequency increases with increasing excitation power density. Since the widths of both state plateaus decrease with increasing excitation power, we can conclude that the transitions from the two states are light induced.

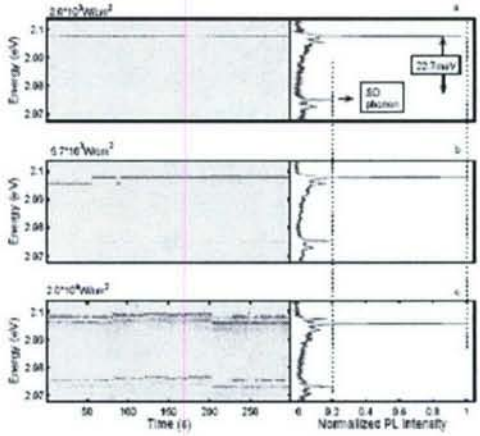

Fig. 23 Spectra from a third NC were recorded continuously with an intergration time of 2 s each. Figure 3(a-c) shows in some NC's, higher laser intensity not only increases the switching frequency, but also makes the states moving randomly. In addition, the ¯gures show there is an additional peak in lower energy side. The energy difference with the exciton peak is 22.7 meV.

Figure 23 (a-c) shows that in some NC's, higher laser intensity not only increases the switching frequency, but also makes the states moving randomly. In addition, the figures show that there is an additional peak in lower energy side with the energy difference 22.7 meV. The energy shifts of the lines are shifting in step. Therefore, we infer that these lines come from a single NC. The right side of Figure 24(a-c) shows the normalized spectrum respectively. We attribute the side peaks to phonon replicas since the ratio of its intensity to the exciton intensity remains constant when the pump intensity changes.

In order to observe more spectral lines, we intergrated over 30 second for each frame in Figure 24. We record 200 measurements continuously with constant temperature and excitation power. Again the energy shifts of the lines are correlated, and therefore, we conclude that these lines come from a single NC. The energy difference between the main line and the satellite lines are 22.7 meV and 25.8 meV, respectively. Also we can see more lines on the lower energy side. The energy

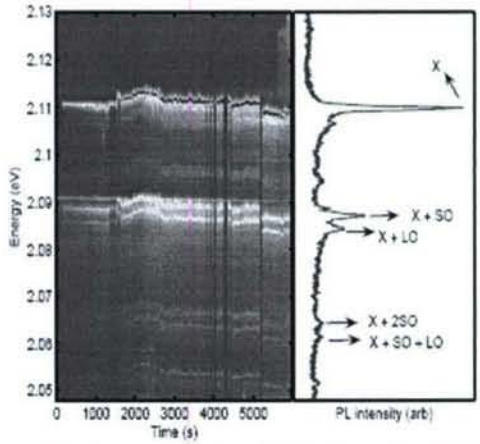

Fig. 24 Spectra from a fourth NC were recorded continuously with an integration time of 30 s each and constant temperature and excitation power. We used a 30s integration time for each frame to see the higher multiplex states which is usually weaker than the exciton peak. Spectrum jitter allows us to group spectral transitions from individual dots. The energy di®erences between the excited state with the ground state are 22.7, 25.8, 45.4, 48.5 meV

differences with the main line are 45.4 meV and 48.5 meV respectively. We identified them as the lines from surface optical(SO) phonons, longitudinal optical (LO) phonons, two SO phonons, and one SO plus one LO phonons.

In summary, we have investigated random switching between two states in the PL from CdSe/ZnS colloidal nanocrystal in PMMA. The commonly observed blinking behavior was suppressed. The spectrum switching behaviors are dominant and some of them are similar to what has been observed in III-V quantum dots. To explain these observations new models going beyond those established in the literature need to be developed. We also found the random energy shift which follows approximately a Lorentzian distribution. Identical jitter patterns allow the unambiguous identication of the emission spectra of single NC's. By means of excitation density dependent spectroscopy the lines are identi¯ed as phonon replica of the exciton transition involving local SO-phonon and LO-phonon modes of the NC. Huang-Rhys factors of *S of about 0.2* are observed.

2. We also continued the development of the heterodyne SNOM (H-NSOM) and applied it for study of various fundamental phenomena in nanophotonic resonant structures and devices. Our first example is on Negative refraction in the photonic crystal lattice. Using a heterodyne scanning near field microscope, we analyzed the phase and amplitude of the electric field of an optical wave across the boundary of a positive to negative refraction media. The photonic crystal acts as an extremely anisotropic material with a negative curvature of its dispersion surface whose shape is clearly resolved experimentally. This extreme anisotropy results in the beam having two peculiar phase properties that do not occur in isotropic media. The first is that the converging wave has diverging wavefronts and after the internal focus, the now diverging wave has converging wavefronts. For this study we prepared a sample shown in Figure 25, where the photonic crystal sample consists of three stages. First, light propagates through a 2μm wide incident ridge waveguide, then it propagates in a 15μm long region of unpatterned silicon-on-insulator (SOI) substrate and finally refracts into a 20μm long PC region. The PC is a square array of holes whose front interface is cut along the <11> direction, as shown in Figure 25A. The sample is excited with TE polarization and has a fundamental mode size of 1.5μm in the ridge waveguide. The beam then diffracts through the homogenous silicon slab region and expands to a size of 6.6μm where it sees the silicon/PC interface. The Bloch mode excited in the PC then negatively refracts and forms an internal focus 3μm behind the interface, which has a transverse size of 2.6μm. Behind the internal focus the beam continues to expand through the PC, as seen in Figure 25B. The second phase anomaly results from the first and is that the negatively refracting

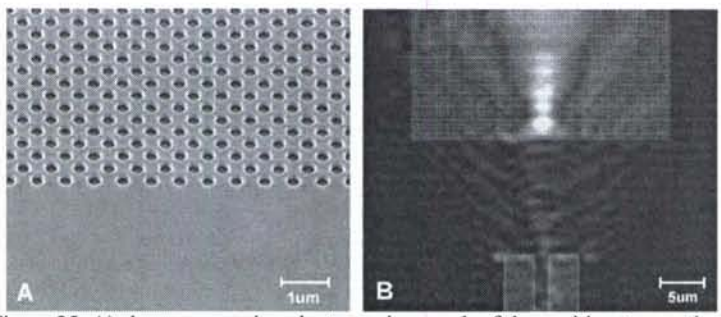

Figure 25. A) shows a scanning electron micrograph of the positive to negative refraction interface. The positive index material consists of an unpatterned region of silicon, which has a thickness of 300nm. The negative refraction material is a square array of holes with a lattice constant of 410nm and a hole diameter of 295nm. B) Shows the field amplitude as measured by a heterodyne SNOM with a low resolution scan. The sample is illuminated with 1560nm light in the TE polarization.

wave has a negative Gouy phase shift. By measuring the full complex values of the guided field, we are able to observe both anomalous phase features of the Bloch wave as well as its dispersion surface.

In another example we study an integrated total internal reflection prism that generates a transversely localized evanescent wave along the boundary between a photonic crystal and an etched out trench. The reflection has previously been described by the symmetry of the Bloch wave field distribution. In this project we show that a tangential momentum matching condition can also describe the reflection. In addition, the Bloch mode propagates through the photonic crystal in a negative refraction regime, which manages diffraction through the prism. A device with three input channels has been fabricated and tested that illuminates different regions of the reflection interface (see Fig. 26). The reflected wave is then sampled by a photonic wire array, where the individual channels are resolved. Heterodyne near field microscopy is used to characterize the spatial phase variation of the evanescent wave and its decay constant. We measured the amplitude and phase of the guided wave at the reflection interface. Figure 27A and its inset show that the amplitude image of the detected field has a peak at the interface and then decays into the air trench, while staying at a roughly constant value in the PC. The wavelength of illumination is 1552 nm, which does not give the tightest field confinement at the interface, but gives a strong signal showing a bright evanescent field. The phase of the field in Fig. 27B shows that along the reflection interface, the phase varies only in the tangential direction. An evanescent field's momentum vector is only real parallel to the interface, so the phase should not progress in any other direction. The inset shows a cross-section of the phase 260 nm behind the interface, which has a period of 1.42 μm, which is below the free space wavelength, indicating that the wave is evanescent. The decay constant of the evanescent field is measured to be 1.20 μms, defined as the e^{-1} location of the field amplitude. The inset is obtained by summing a 10 μm wide field along the boundary, and plotting the summation as a function of vertical distance. The summation averages field values over several unit cells of the PC and results in a smooth curve. Field values in the HNSOM image are sampled at an interval of 260 nm, so there are 4-5 measurements in the e^{-1} decay region. A near-field object is convolved with the collection tip, in this case 200 nm. This convolution blurs sharp features by approximately this amount, which increases the measured decay distance. Along the interface, the amplitude is modulated by the surface periodicity of the PC, $\sqrt{3}a$, but this does not describe the phase progression, as we will see by looking at the tangential phase profile.

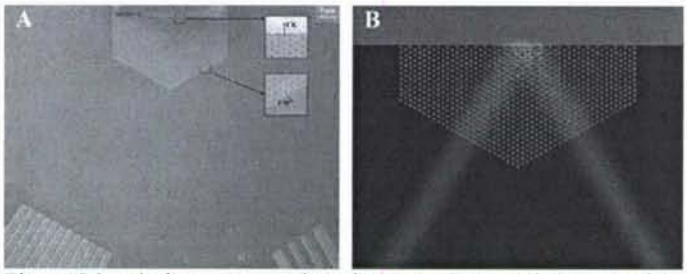

Figure 26. A) shows a scanning electron micrograph (SEM) of the fabricated device. The insets show the crystal terminations for the prism input and reflection interfaces. The front half of the prism is surrounded by silicon slab, and behind the prism is an etched out air trench. B) shows a numerical simulation of the time averaged square of the E_z (TM) field. The wave is incident from the bottom right and exits the bottom left. The numerically simulated device is three times smaller than the fabricated device, so diffraction is negligible.

The phase image in Fig. 6 shows a coherent wave incident into the boundary from the PC and along the interface. The tangential momentum of these two waves is equal according to the boundary condition. By taking a cross-section of the phase image just beyond the interface in

the gap, the spatial period of the wave is observed to be 1.42 μm, which gives k_{ev}=1.09k_{air}. The decay constant of an evanescent wave can be predicted from its momentum by the expression $D = 1/\sqrt{k_{ev}^2 - k_{air}^2}$. Using k_{ev}=1.09k_{air}, the decay constant is expected to be 570 nm, which is larger than the measured value of 1.2 μm. Because the field is spatially confined, there is a spectrum of transverse momentum values at the boundary. Lower spatial frequencies decay slower into the air region, so they have greater influence at large distances from the interface. In order to better understand the spectrum of the evanescent wave, we can Fourier analyze the measured complex field. This method also gives insight into the reason for measuring a larger D.

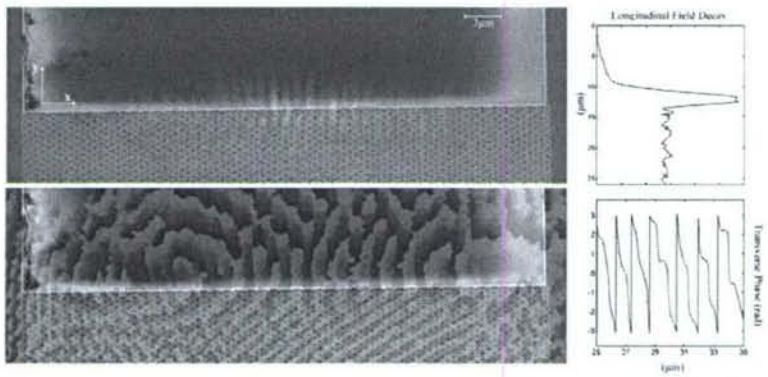

Figure 27. The amplitude and phase images along the reflection interface collected by the HNSOM superimposed on the SEM image to show the geometry. The inset to the amplitude image shows an averaged field amplitude curve plotted vs. **y**. The inset to the phase image shows the evanescent field phase one sample above the interface in the air region plotted vs. **x**.

Figure 28 is the numerical Fourier transform of the measured complex field from a 15 x 15 μm scanning area centered at the reflection edge. The brightest feature in the spectrum is the incident Bloch wave, $k_{i\text{-}PC}$, and is located in the upper left region indicating that its phase progresses in that direction. By measuring the magnitude of $k_{i\text{-}PC}$, the effective index of the primary momentum distribution is estimated to be 2.2. As long as this value is larger than 2.0, the Bloch wave will TIR at the boundary when the incident angle is 30°. This value agrees with the numerical prediction from FDTD of 2.35 and further illustrates the close momentum match between the slab mode and the PC mode, which has an index of 2.54. It is also evident that the momentum distribution is flat indicating that the wave is in a slow diffraction regime. This region of the spectrum is labeled A.

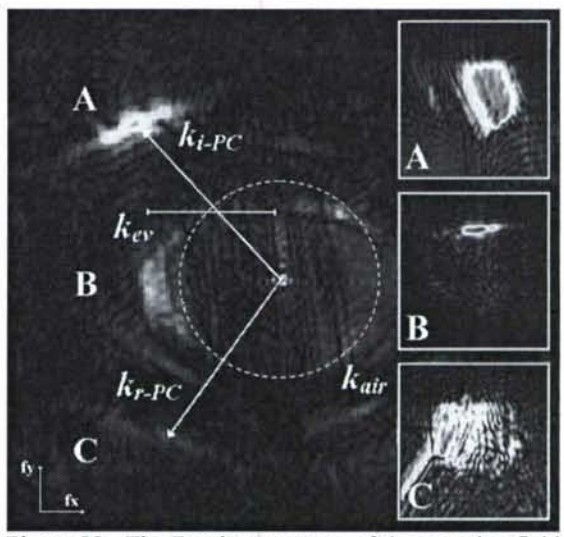

Figure 28. The Fourier spectrum of the complex field values collected by the HNSOM. The arrows show the incident Bloch wave, $k_{i\text{-}PC}$, the reflected Bloch wave, $k_{r\text{-}PC}$, and the evanescent wave, k_{ev}. The dotted circle shows the air light line at 1552 nm. The insets show the windowed regions after being inverse transformed back to the spatial domain.

At the same tangential momentum, but along the $\mathbf{f_x}$-axis, is the second brightest region labeled B. The spectrum of the evanescent wave is expected to be in region B because the only real component of its momentum is along the tangent of the interface. From the figure, the evanescent

spectrum lies just beyond the air light line and has energy from 1.0-1.3k_{air}. The momentum components only slightly larger than k_{air} will decay very slowly and are responsible for the larger than expected measured value of D. The higher end of the k_{ev} spectrum compares well with the value expected by numerical simulation. Region C contains the reflected wave spectrum, which is surprising weak considering the large efficiency observed in far-field measurements.

Each region can be windowed and inverse Fourier transformed back to the spatial domain to view where that piece of the spectrum is located. The inset labeled A shows that this region is in fact the incident PC mode, which starts at the PC input facet and ends at the reflection interface. Region C, though weaker, shows the reflected PC wave starting at the reflection interface and ending at the PC output facet. Region B, which is the evanescent wave, is confined to the reflection edge. The windowed spatial field distribution has less resolution, but makes it possible to isolate different components of the detected field. The near-field microscope efficiently collects the PC prism's evanescent field as can be seen by the low noise floor in inset B compared to the other insets. In summary, a PC TIR prism has been demonstrated that acts as an efficient evanescent wave source that is integrated onto a silicon platform. Different resolvable regions along the PC to air boundary can be illuminated due to diffraction management and the presence of input and output waveguide arrays. These channels spatially overlap in the prism so consequently perform a function that is difficult to obtain in conventional integrated optics. The device can in the future be scaled up, where the number of resolvable channels will be dictated by the aperture of the prism divided by the beam size, which can be on the order of 1-2 λ. In addition, the near-field performance of this device has been characterized. We have directly measured the phase and amplitude distributions of the generated evanescent wave. Although previously the PC's inability to couple across an air boundary has been described by mode symmetry, we have shown here that transverse momentum conservation can also describe the reflection. These arguments have been made using the Fourier spectrum of both numerical and experimental data. The strong presence of the detected evanescent field imply that the PC TIR prism might allow efficient and flexible evanescent wave coupling, imaging, and sensing functionalities.The device presents a means to generate an evanescent wave with high efficiency and a localized extent into a parallel system on an integrated platform.

3. We also started a new direction in Si Nanophotonics that we call "free space optics on a chip". Besides a number of new near field optical phenomena that we investigated numerically and are in the process of fabrication and testing, we have demonstrated a new "Inhomogeneous Metamaterial with Space-variant Polarizability" which is extremely useful for mode matching on a Si chip. The design was performed using both rigorous coupled wave (plane wave spectral) analysis and an approximate effective index theory developed by Rytov (with proper modifications). The

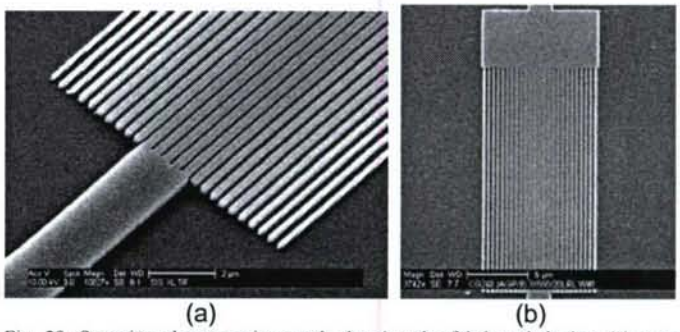

(a) (b)

Fig. 29: Scanning electron micrograph showing the fabricated device: (a) a top view of the entire structure. (b) a magnified slanted view showing part of the slab lens and the output waveguide.

designed nanostructure was fabricated using our e-beam lithography and reactive ion beam etching (see Fig. 29). The fabricated devices were characterized with the H-NSOM tool. The experimental results shown in Fig. 30 confirm our design and fabrication process, demonstrating a slight discrepancy due to lithographic proximity effects during fabrication of features less than 100nm. This study clearly demonstrated the value of closing the loop between design, fabrication and testing-nanophotonics process pioneered in our group.

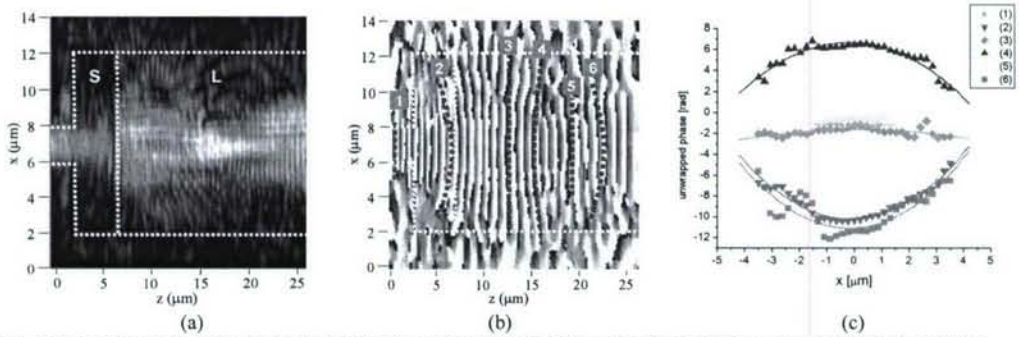

(a) (b) (c)

Fig. 30: Experimental results obtained with the Heterodyne Near field Scanning Optical Microscope (H-NSOM). (a) The amplitude and (b) the phase of the optical field in the region that includes the input waveguide, the non-patterned slab ("S") and large portion of the slab lens section ("L"). The dashed vertical white lines mark the boundaries between the various sections. Light is propagating from left to right. (c) Cross sections showing phase profile at several planes along the device. The planes are marked in Fig. 5b.

4. We further enhanced Si Nanophotonics research by exploiting a single lithographic step in creating geometries on the sub-100 nm scale that realize complex nanophotonic structures, devices and circuits. A simple example we used for the first validation of our ideas is a one dimensional photonic crystal waveguide with a single mode defect that implements a resonant filter. We implement vertical side wall modulation in a silicon waveguide implemented with standard SOI. Transmission resonant filters in a waveguide with vertical gratings have been realized in silicon on insulator (SOI) wafers (see Fig. 31a).

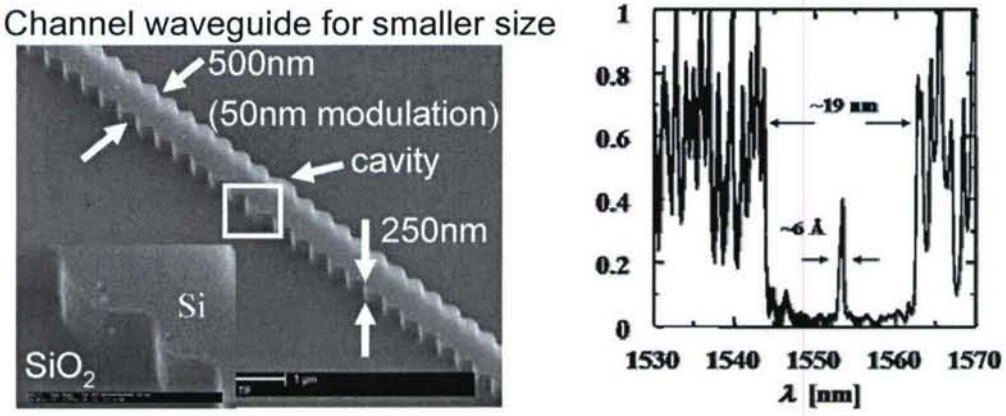

Fig.31 (a) SEM micrographs of the whole device and its inset showing resonant filter device. Dotted rectangle shows the area defined at × 1000 magnification and (b) Measured transmission spectra from the fabricated devices

Experimental studies of fabricated devices show a broad stopband of ~19 nm with a narrow transmission band of ~0.6 nm (see Fig 31b). The developed fabrication procedures show very good surface quality which is also indicated by the measured value of the single mode cavity Q of about 3, 000. These resonant cavities are useful for laser cavities, switches, modulators, detectors, and tunable filters.

5. We also continued our studies of the surface plasmon polaritons in the 2-D nanohole arrays. Specifically we continued the studies of various modes excitation, interaction, and detection with special emphasis on integrating plasmonics with optofluidics and gain medium. These studies are currently being investigated in conjunction with the sensing applications.

4. Personnel Supported

Y. Fainman, PI, Professor (UCSD)
Lu Sham, co-PI, Professor (UCSD)
Charles W. Tu, co-PI, Professor (UCSD)
Kevin Tetz, Research Assistant (UCSD)
Maxim Abashin, Research Assistant (UCSD)
Yaoming Shen, Research Assistant (UCSD)
Vladimir Odnoblyudov, Research Assistant (UCSD)
Lin Pang, Postdoctoral Researcher (UCSD)
Hiroshi Ajiki, Postdoctoral Researcher (UCSD)
Wang Yao, Graduate Research Assistant (UCSD)
Robbie Saperstein, Graduate Research Assistant (UCSD)
Kaz Ikeda, Graduate Research Assistant (UCSD)

5. Publications

1. A. Ajiki, W. Yao, L. J. Sham, "Enhancement of the Kerr effect for a quantum dot in a cavity", Superlattices and Microstructures **34**, 213-217 (2003).

2. W. Yao, Renbao Liu, and L. J. Sham, "Nanodot-cavity electrodynamics and photon entanglement", Phys. Rev. Lett. **92**, 217402 (2004), 4 pages.

3. W. Yao, Renbao Liu, and L. J. Sham, "Quantum network of local qubits mediated by single photon pulses of arbitrary shape: state transfer and entanglement creation", Online arXiv:quant-ph/0407060, submitted for publication.

4. Renbao Liu, W. Yao, and L. J. Sham, "Ultrafast initialization and QND-readout of a spin qubit via control of nanodot-vacuum coupling", Online arXiv:condmat/0408148, submitted for publication.

5. L. Pang, W. Nakagawa, and Y. Fainman, " Fabrication of opticsl structures using SU-8 photoresist and chemically assisted ion beam etching," Opt. Eng., vol. 42, pp. 2912-2917, 2003

6. L. Pang, W. Nakagawa, and Y. Fainman, " Fabrication of two-dimensional photonic crystals with controlled defects by use of multiple exposures and direct write," Applied Optics, vol. 42, pp. 5450-5456, 2003

7. A. Nishikawa, Y.G. Hong, and C.W. Tu, "Temperature dependence of optical properties of $Ga_{0.3}In_{0.7}N_xAs_{1-x}$ quantum dots grown on GaAs (001)", J. Vac. Sci. Technol. B, vol.22, no.3, pp.1515-17, May 2004.

8. Y.G. Hong, A. Nishikawa, and C.W. Tu, "Effect of nitrogen on the optical and transport properties of $Ga_{0.48}In_{0.52}N_yP_{1-y}$ grown on GaAs(001) substrates", Appl. Phys. Lett., vol.83, no.26, pp.5446-8, 29 Dec. 2003.

9. Y.G. Hong, A. Nishikawa, and C.W. Tu, "Similarities between $Ga_{0.48}In_{0.52}N_yP_{1-y}$ and $Ga_{0.92}In_{0.08}N_yAs_{1-y}$ grown on GaAs (001) substrates", J. Vac. Sci. Technol. B, vol.22, no.3, pp.1495-8, May 2004.

10. A. Nishikawa, Y.G. Hong, and C.W. Tu, "The effect of nitrogen on self-assembled GaInNAs quantum dots grown on GaAs", Physica Status Solidi B, vol.240, no.2, pp.310-13, Nov. 2003.

11. A. Nishikawa, Y.G. Hong, and C.W. Tu, "Effects of thermal annealing on $Ga_{0.3}In_{0.7}N_xAs_{1-x}$ QDs grown on GaAs (001)", 2003 Int'l Symp. Comp. Semicon., pp.55-60, 2004.

12. A. Nishikawa, Y.G. Hong, and C.W. Tu, "Extension of emission wavelength of GaInNAs QDs grown on GaAs (001)", 2003 Int'l Conf. Indium Phosphide and Rel. Mat'l, Conf. Proc, pp.359-60, 2004.

13. Beom-hoan O, Chul-Hyun Choi, Soo-Beom Jo, Min-Woo Lee, Dong-Gue Park, Byeong-Gwon Kang, Sun-Hyung Kim, Rong Liu, Yang Yang Li, Sailor MJ, Fainman Y. Novel form birefringence modeling for an ultracompact sensor in porous silicon films using polarization interferometry. [Journal Paper] IEEE Photonics Technology Letters, vol.16, no.6, June 2004, pp.1546-8. Publisher: IEEE, USA.

14. M. P. Nezhad, K. Tetz, and Y. Fainman,"Gain assisted propagation of surface plasmon polaritons on planar metallic waveguides," Opt. Express 12, 4072-4079 (2004)

15. M. P. Nezhad, K. Tetz, and Y. Fainman, "Gain assisted propagation of surface plasmon polaritons on planar metallic waveguides," Opt. Express 12, 4072-4079 (2004)
16. M. A. Alvarez-Cabanillas, F. Xu, Y. Fainman, "Modeling microlenses by use of vectorial field rays and diffraction integrals," Applied Optics, vol.43, no.11, pp.2242-50, 2004.
17. W. Nakagawa, Y. Fainman, "Tunable optical nanocavity based on modulation of near-field coupling between subwavelength periodic nanostructures," IEEE Journal of Selected Topics in Quantum Electronics, vol.10, no.3, pp.478-83, 2004.
18. U. Levy and Y. Fainman, "Dispersion properties of inhomogeneous nanostructures," J. Opt. Soc. Am. A., 21, 881-889 (2004).
19. U. Levy, C. H. Tsai, L. Pang and Y. Fainman, "Engineering space-variant inhomogeneous media for polarization control," Opt. Lett., 29, 1718-1720 (2004)
20. U. Levy, C. H. Tsai, H. C. Kim and Y. Fainman, "Design, fabrication and characterization of subwavelength computer-generated holograms for spot array generation," Opt. Express, **12,** 5345 – 5355 (2004).
21. K Campbell, A. Groisman, U. Levy, L. Pang, S.hayan Mookherjea D. Psaltis and Y. Fainman, "A microfluidic 2×2 optical switch," Appl. Phys. Lett. **85,** 6119-6121 (2004).
22. R. E. Saperstein, D. Panasenko, Y. Fainman, ""Demonstration of a microwave spectrum analyzer based on time-domain optical processing in fiber" Opt. Lett. **29,** 501-503 (2004).
23. C. Chen, K. Tetz, W. Nakagawa, and Y. Fainman, "Wide Field of View GaAs/AlxOy 1-D Photonic Crystal Filter", Appl. Opt. Vol. 44, no. 8, pp. 1503-1511 (2005).
24. U. Levy, M. Nezhad, H. C. Kim, C. H. Tsai, L. Pang and Y. Fainman, "Implementation of graded index medium using subwavelength structures with graded fill factor," J. Opt. Soc. Am. A. **22**, 724-733 (2005).
25. L. Pang, Y.-M. Shen, K. Tetz and Y.Fainman, 'PMMA quantum dots composites fabricated via use of pre-polymerization,' Opt. Exp.13, 44-49 (2005).
26. L. Pang, M. Nezhad, U. Levy, C.-H. Tsai, and Y. Fainman, 'Form birefringence structure fabrication in GaAs by use of SU-8 as dry etching mask', Appl. Opt. **44**, 2377-2381 (2005).

During Period 2004-2005:

27. K. Tetz, R. Rokitski, M. Nezhad, and Y. Fainman, "Excitation and Direct Imaging of Surface Plasmon Polariton Modes in a Two-dimensional Grating", Appl. Phys. Lett. vol.86, no.11, 111110 (2005). Also Featured in *Editor's Choice: Highlights of recent literature*, Science, vol. 307, p. 1841 (2005).
28. C. Chen, L. Pang, C. Tsai, U. Levy, and Y. Fainman, Compact and integrated TM-pass waveguide polarizer, Opt. Express **13**, 5347-5352 (2005).
29. D. Panasenko, S. Putilin and Y. Fainman, Tunable spectral interferometry for broadband phase detection using pair of Optical Parametric Amplifiers, JOSA B, **22**, 922-929 (2005)

30. Levy U, Hyo-Chang Kim, Chia-Ho Tsai, Fainman Y. Near-infrared demonstration of computer-generated holograms implemented by using subwavelength gratings with space-variant orientation. *Optics Letters, vol.30, no.16, 15 Aug. 2005, pp.2089-91*
31. N. Alic, G.C. Papen, R.E. Saperstein, L.B. Milstein, and Y. Fainman, Signal Statistics and Maximum Likelihood Sequence Estimation in Intensity Modulated Fiber Optic Links Containing a Single Optical Pre-amplifier Opt. Expr., **13**, 4568-4579 (2005).
32. R. Saperstein, N. Alic, D. Panasenko, R. Rokitski, and Y. Fainman, Time-domain waveform processing by chromatic dispersion for temporal shaping of optical pulses, J. Opt. Soc. Am. B **22**, 2427-2436 (2005).
33. LinPang, KevinTetz,YaomingShen,Chyong-HuaChen,andYeshaiahuFainman, "Photosensitive quantum dot composites and their applications in optical structures," J.Vac.Sci.Technol. B23, 6, pp. 2413- 2418, 2005
34. L. Pang, C.H Tsai, and Y. Fainman, 'Influence of chlorine on etched sidewall in chemically assisted ion beam etching with SU-8 as mask,' Opt. Eng. 44, (6) 2005.
35. C. Chen, K. Tetz, and Y. Fainman, Resonant-Cavity-Enhanced (RCE) Quantum efficiency PIN photodiode with flat-top passband filter functionality, Appl Opt. Vol. **44**, 6131-6140 (2005).
36. P. Tortora, M. Abashin, I. Marki, W. Nakagawa, L.Vaccaro, M. Salt, HP. Herzig, U. Levy, Y. Fainman, "Observation of amplitude and phase in ridge and photonic crystal waveguides operating at 1.55 mu m by use of heterodyne scanning near-field optical microscopy," *Optics Letters, vol.30, no.21, pp.2885-71, 2005*
37. R. Rokitski, KA. Tetz, Y. Fainman, "Propagation of femtosecond surface plasmon polariton pulses on the surface of a nanostructured metallic film: Space-time complex amplitude characterization," *Physical Review Letters, vol.95, no.17, 21 Oct. 2005, pp.177401/1-4*

During Period 2005-2006:

38. Wang Yao, Ren-Bao Liu, and L. J. Sham, "Theory of Control of the Spin-Photon Interface for Quantum Networks", *Phys. Rev. Lett.* **95**, 030504 (2005), 4 pages. RESEARCH ARTICLE
39. Ren-Bao Liu, Wang Yao, and L. J. Sham, "Coherent control of cavity quantum electrodynamics for quantum nondemolition measurements and ultrafast cooling", Phys. Rev. B **72,** 081306 (R) (2005), 4 pages. RESEARCH ARTICLE
40. Wang Yao, Ren-Bao Liu, and L. J. Sham, "Theory of control of interfacing dynamics between stationary and flying qubit", J. Opt. B: Quantum Semiclass. Opt. **7,** S318-S325 (2005). 8 pages. RESEARCH ARTICLE
41. Wang Yao, Ren-Bao Liu, and L. J. Sham, "Theory of electron spin decoherence by interacting nuclear spins in a quantum dot", Phys. Rev. B **74**, 195301 (2006). 11 pages. RESEARCH ARTICLE
42. Wang Yao, Ren-Bao Liu, and L. J. Sham, "Restoring Coherence Lost to a Slow Interacting Mesoscopic Spin Bath", Phys. Rev. Lett. **98**, 077602 (2007). 4 pages. RESEARCH ARTICLE
43. S. Suraprapapich, S. Panyakeow, and C.W. Tu, "The effect of arsenic species on the formation of (Ga)InAs nanostructures after partial-capping-and-regrowth", accepted for publication in *Appl. Phys. Lett.* (2007).
44. S. Suraprapapich, Y.M. Shen, V.A. Odnoblyudov[a], Y. Fainman, S. Panyakeow, and C.W. Tu, "Self-Assembled Lateral Bi-Quantum-Dot Molecule Formation by Gas-Source Molecular Beam Epitaxy", accepted for publication in *J. Crystal Growth* (2007).

45. Klemens G, Chyong-Hua Chen, Yeshaiahu Fainman. Design of optimized dispersive resonant cavities for nonlinear wave mixing. [Journal Paper] *Optics Express, vol.13, no.23, 14 Nov.* 9388-9397 , *2005*
46. M. Abashin, P. Tortora, I. Marki, U. Levy, W. Nakagawa, L. Vaccaro, H. Herzig, and Y. Fainman, Near-field characterization of propagating optical modes in photonic crystal waveguides, Optics Express **14**, 1643-1657 (2006).
47. U. Levy, K. Campbell, A. Groisman, S. Mookherjea, and Y. Fainman, On-chip microfluidic tuning of an optical microring resonator, Appl. Phys. Lett., **88**, 111107-111109 (2006).
48. C-H Tsai, U. Levy, L. Pang, and Y. Fainman, Form-birefringent space-variant inhomogeneous medium element for shaping point-spread functions, Appl. Opt. **45**, 1777-1784 (2006).
49. K. A. Tetz, P. Lin, Y. Fainman, High-resolution surface plasmon resonance sensor based on linewidth-optimized nanohole array transmittance, *Optics Letters,.**31**, 1528-30, 2006*
50. G. Klemens and Y. Fainman, Optimization-based calculation of optical nonlinear processes in a micro-resonator, Opt. Express **14**, 9864-9872 (2006).
51. K. Ikeda and Y. Fainman, Nonlinear Fabry-Perot resonator with a silicon photonic crystal waveguide Opt. Lett. **31**, 3486-3488 (2006).
52. P. Lin, K. A. Tetz, Y. Fainman "Observation of the splitting of degenerate surface plasmon polariton modes in a two-dimensional metallic nanohole array," Applied Physics Letters 90, 111103 (2007)
53. Lomakin V, Fainman Y, Urzhumov Y, Shvets G. Doubly negative metamaterials in the near infrared and visible regimes based on thin film nanocomposites. *Optics Express, vol.14, no.23, Nov. 2006*
54. Fainman Y, Tetz K, Rokitski R, Lin Pang. Surface plasmonic fields in nanophotonics. *Optics & Photonics News, vol.17, no.7-8, July-Aug. 2006, pp. 24-9.*
55. Schonbrun E, Qi Wu, Park W, Yamashita T, Summers CJ, Abashin M, Fainman Y. Wave front evolution of negatively refracted waves in a photonic crystal. *Applied Physics Letters, vol.90, no.4, 22 Jan. 2007, pp. 41113-1-3.*
56. Hyo-Chang Kim, Kazuhiro Ikeda, and Yeshaiahu Fainman Resonant waveguide device with vertical gratings, Optics Letters, Vol. 32, Issue 5, pp. 539-541, 2007

6. Interactions/transitions

a. Meetings, Conferences, Seminars, Proceedings

1. Y. Fainman, " Nanophotonic materials and devices," Photonics West, SPIE Conference, San Jose, ,January 25-29, 2003. **(Invited)**

2. Y. Fainman, "Ultrafast Information Processing with Optical Nonlinearities," CLEO/QELS, June 1-6, 2003, Baltimore, Maryland, , **(Tutorial)**

3. Y. Fainman, D. Panasenko, R. Rokitski, D. Marom, K. Oba, Y. Mazurenko, and P. C. Sun, "Ultrafast Information Processing with Optical Nonlinearities," presented at Optics in Computing conference, Washington, DC, June 18-20, 2003. Optics in Computing (Trends in Optics and Photonics Series Vol.90). Optical Soc. of America. 2003, pp.100-2. **(Invited)**

4. Y. Fainman, " Nanophotonic Materials and Devices for Optical System Integration," DARPA Topical Meeting on Optical Photonic Bandgap Research, January 22-23, 2003. **(Invited)**

5. L. Pang, W. Nakagawa, C.-H. Tsai, and Y. Fainman, 'Fabrication of 2D photonic crystal using multiple exposures', Proc. SPIE 5181, 223 (2003)

6. M. P. Nezhad, C. Tsai, L. Pang, W. Nakagawa, G. Klemens, and Y. Fainman , "Form birefringent retardation plates in GaAs substrates: design, fabrication, and characterization", Proc. of SPIE, vol. 5225, Nano- and Micro-Optics for Information Systems, Louay A. Eldada, Editor, October 2003, pp. 69-77

7. Nesci A, Fainman Y. Complex amplitude of an ultrashort pulse with femtosecond resolution in a waveguide using a coherent NSOM at 1550 nm. [Conference Paper] SPIE-Int. Soc. Opt. Eng. Proceedings of Spie - the International Society for Optical Engineering, vol.5181, no.1, 2003, pp.62-9.

8. Panasenko D, Rokitski R, Alic N, Marom DM, Mazurenko YT, Pang Chen Sun, Fainman Y. Real-time synthesis and detection of ultrafast optical waveform. [Conference Paper] SPIE-Int. Soc. Opt. Eng. Proceedings of Spie - the International Society for Optical Engineering, vol.4978, no.1, 2003, pp.58-69. **(Invited)**

9. C. H. Tsai, U. Levy, L. Pang, Y. Fainman, "Fabrication and characterization of GaAs-based space-variant inhomogeneous media for polarization control at 10.6um", Proc. SPIE, Nanoengineering: Fabrication, Properties, Optics, and Devices, Vol.5515, pp.142-149 (2004)

10. R. E. Saperstein, D. Panasenko, Y. Fainman, "Demonstration of a RF-photonic spectrum analyzer using ultrafast optical pulses," in Technical Digest of 2003 Frontiers in Optics, The 87th OSA Annual Meeting and Exhibit (Omnipress, 2003), Session WII4

11. R. E. Saperstein, D. Panasenko, Y. Fainman, "Demonstration of a microwave spectrum analyzer using time-domain processing in optical fibers" in 2003 IEEE LEOS Annual Meeting Conference Proceedings (IEEE, Piscataway, NJ, 2003), 931-932

12. Fainman Y, Panasenko D, Rokitski R, Saperstein R, Marom DM, Mazurenko YT, Sun PC. Applications of optical nonlinearities for signal processing. [Conference Paper] 2003 IEEE LEOS Annual Meeting Conference Proceedings (IEEE Cat. No.03CH37460). IEEE. Part vol.1, 2003, pp.262-3 vol.1. Piscataway, NJ, USA.**(Invited)**

13. Nesci A, Fainman Y. Complex amplitude of an ultrashort pulse in a waveguide measured with a coherent, femtosecond resolution NSOM at 1550 nm. [Conference Paper] 2003 IEEE LEOS Annual Meeting Conference Proceedings (IEEE Cat. No.03CH37460). IEEE. Part vol.1, 2003, pp.49-50 vol.1. Piscataway, NJ

14. Ambs P, Bigue L, Fainman Y, Binet R, Collineau J, Lehureau J-C, Huignard J-P. Image reconstruction using electrooptic holography. 2003 IEEE LEOS Annual Meeting Conference

Proceedings (IEEE Cat. No.03CH37460). IEEE. Part vol.1, 2003, pp.179-80 vol.1. Piscataway, NJ, USA.**(Invited)**

15. Nakagawa W, Tetz K, Fainman Y. Design of near-field optical nanostructures for enhanced second-harmonic generation. [Conference Paper] Quantum Electronics and Laser Science (QELS). Postconference Digest (IEEE Cat No.CH37420-TBR). Optical Soc. of America. 2003, pp.2 pp.. Washington, DC

16. Y. Fainman," Ultrafast Signal Processing using optical nonlinearities," Optics in Computing, Switzerland, April 2004.**(Invited)**

17. Levy U, Chia-Ho Tsai, Nezhad M, Nakagawa W, Chen C-H, Tetz KA, Pang L, **Fainman** Y. Nanophotonics: materials and devices. [Conference Paper] SPIE-Int. Soc. Opt. Eng. Proceedings of Spie - the International Society for Optical Engineering, vol.5359, no.1, 6 July 2004, pp.126-44. USA

18. R. E. Saperstein, N. Alic, D. Panasenko, R. Rokitski, Y. Fainman, "Time-Domain Optical Processing using Chromatic Dispersion for Ultrashort Pulse Shaping" presented at 2004 IEEE LEOS Annual Meeting, Nov. 7-11, 2004 Rio Mar, Puerto Rico

19. M. P. Nezhad, K. Tetz, U. Levy and Y. Fainman "Propagation of Surface Plasmon Polaritons on the Boundary of a Metal and a Gain Medium," presented at 2004 IEEE LEOS Annual Meeting, Nov. 7-11, 2004 Rio Mar, Puerto Rico

20. K. Tetz, R. Rokitski , M. P. Nezhad , and Y. Fainman, "Excitation and Direct Imaging of Surface Plasmon Polariton Modes in the Near-Infrared," presented at 2004 IEEE LEOS Annual Meeting, Nov. 7-11, 2004 Rio Mar, Puerto Rico

21. **Fainman** Y, Tetz K, Levy U, Nakagawa W, Tsai C-H, Chen C-H, Pang L, Nezhad M, Nesci A, Sun PC. Nanophotonics for optoelectronic system integration. [Conference Paper] *2004 IEEE LEOS Annual Meeting Conference Proceedings (IEEE Cat. No.04CH37581). IEEE. Part Vol.1, 2004, pp.45-6 Vol.1. Piscataway, NJ, USA.* **(Invited)**

22. **Fainman** Y, Saperstein R, Rokitski R, Panasenko D, Alic N, Marom D, Mazurenko Y, Sun PC. Signal processing, imaging and cryptography with ultrashort laser pulses. [Conference Paper] *2004 IEEE LEOS Annual Meeting Conference Proceedings (IEEE Cat. No.04CH37581). IEEE. Part Vol.2, 2004, pp.929-30 Vol.2. Piscataway, NJ, USA* **(Invited)**

23. Lin Pang, Levy U, Campbell K, Groisman A, Mookarjee S, Psaltis D, **Fainman** Y. A microfluidic 2*2 optical switch. [Conference Paper] *2004 IEEE LEOS Annual Meeting Conference Proceedings (IEEE Cat. No.04CH37581). IEEE. Part Vol.1, 2004, pp.124-5 Vol.1. Piscataway, NJ, USA*
24. Alic N, Papen GC, Fainman Y. Performance of maximum likelihood sequence estimation with different modulation formats. [Conference Paper] 2004 IEEE/LEOS Workshop on Advanced Modulation Formats (IEEE Cat. No.04EX834). IEEE. 2004, pp.49-50. Piscataway, NJ, USA.

25. Alic N, Papen GC, **Fainman** Y. Theoretical performance analysis of maximum likelihood sequence estimation in intensity modulated short-haul fiber optic links. [Conference Paper] *2004 IEEE LEOS Annual Meeting Conference Proceedings (IEEE Cat. No.04CH37581). IEEE. Part Vol.2, 2004, pp.753-4 Vol.2. Piscataway, NJ, USA.* presented at 2004 IEEE LEOS Annual Meeting, Nov. 7-11, 2004 Rio Mar, Puerto Rico **(Postdeadline paper)**

During Period 2004-2005:

27. N. Alic, G.C. Papen, L.B. Milstein, P.H. Siegel and Y. Fainman,"Performance Bounds of MLSE in Intensity Modulated Fiber Optic Links" TIWDC 2004, A Topical Meeting on Optical Communication Theory and Techniques, paper IV.5 (Tyrrhenian International Workshop on Digital Communications) Pisa, Italy, Oct 1-2, 2004. A book, rather than a conference proceedings, was published by Springer containing the papers from the workshop. Book title: Optical Communication Theory and Techniques (Edited by Enrico Forestieri), Springer 2005. pp. 197-203.
28. Yaoming Shen, Lin Pang, Tetz KA, **Fainman** Y. Characterization of PMMA quantum dot composite fabricated by pre-polymerizing method. [Conference Paper] *SPIE-Int. Soc. Opt. Eng. Proceedings of Spie - the International Society for Optical Engineering, vol.5510, no.1, 2004, pp.33-40. USA.*
29. Levy U, Chia-Ho Tsai, Lin Pang, **Fainman** Y. Polarization transformations by engineering space-variant inhomogeneous media on subwavelength scale. [Conference Paper] *Conference on Lasers and Electro-Optics (CLEO). IEEE. Part vol.2, 2004, pp.1 pp. vol.2. Piscataway, NJ, USA*
30. E. Saperstein, X. B. Xie, P. K. L. Yu, and Y. Fainman. "Demonstration of a microwave spectrum analyzer based on time-domain processing of ultrashort pulses." Conference on Lasers and Electro-Optics, (2005) CTuAA4
31. Tortora, M. Abashin, W. Nakagawa Investigation of the spectral characteristics of photonic crystal waveguides with heterodyne scanning near-field optical microscopy NPIS 2005 Conf. Proc. **NThC2**
32. U. Levy, C.-H. Tsai, M. Nezhad, L. Pang, Y. Fainman, Subwavelength based components for beam shaping applications," OSA annual meeting, Rochester, 2004, paper FWQ3
33. U. Levy, H. C. Kim, S. Mookherjea, K. Ikeda and Y. Fainman, "Nanophotonics for optical delay," Phot. West, 2005, San Jose, CA, paper 5735-13(**invited paper**)
34. U. Levy, C. H. Tsai, H. C. Kim, L. Pang and Y. Fainman, "Design, Fabrication and Characterization of Artificial Dielectrics for Polarization Transformations and Beam Shaping Applications," OSA Topical Meeting on Nanophotonics for Information Systems, San Diego, 2005, paper NWB5.
35. U. Levy, Y. Fainman, A. Krishnamoorthy and J. Cunningham, "Novel Slab lens based on artificial graded index medium," OSA Topical Meeting on Information Photonics, Charlotte, 2005, paper IWB2.
36. **K. A. Tetz**, R. Rokitski, Y. Fainman; "Spatio-Temporal Characterization of Ultrashort Surface Plasmon Polariton Pulses Propagating in Two-Dimensional Nanohole Arrays", OSA NPIS, San Diego, CA, April 2005.
37. M. Abashin, P. Tortora, U. Levy et al. *Nearfield Investigation of Mode Structure in Photonic Crystal Waveguides* CLEO/QELS 2005 Conf. Proc. **QTuK3**

38. Y. Fainman, R. Saperstein, R. Rokitski, K. Tetz, D. Panasenko, N. Alic, D. Marom, Y. Mazurenko, and P. C. Sun "Information processing with ultrashort laser pulses" 14-th International Laser Physics Workshop (LPHYS'05), July 4-8, 2005, Kyoto, Japan (**Invited)**
39. Yeshaiahu Fainman, Kevin A. Tetz, Rostislav Rokitski, and Maziar Nezhad, "Ultra short surface plasmon polaritons in photonic crystal structures," IQEC-CLEO-PR2005 July 13, 2005(**Invited)**
40. Y. Fainman, R. Saperstein, R. Rokitski, K. Tetz, D. Panasenko, N. Alic, D. Marom, Y. Mazurenko, and P. C. Sun "Information processing with ultrashort laser pulses," Laboratory for Physical Sciences, University of Maryland, July 20, 2005 (**Invited)**
41. Y. Fainman, A. Groisman, S. Mookherjea, U. Levy, L. Pang, K. Campbell, K. Tetz, M. Nezhad, R. Rokitski and D. Psaltis, "Adaptive and Tunable Optics with Microfluidics" Optical Information Systems III, Optics and Photonics - SPIE, July 31-August 4, 2005, San Diego, California
42. Y. Fainman, K. Tetz, U. Levy, W. Nakagawa, C.-H. Tsai, C.-H. Chen, L. Pang, M. Nezhad, M. Abashin, A. Nesci, and P. C. Sun, "Nanophotonics for Optoelectronic Systems Integration" Optics in the South-East, Georgia Tech, October 8, 2005(**Invited)**
43. Y. Fainman, K. Tetz, U. Levy, W. Nakagawa, C.-H. Tsai, C.-H. Chen, L. Pang, M. Nezhad, M. Abashin, A. Nesci, and P. C. Sun, "Nanophotonic Materials and Devices for Information Systems Integration" presented at the OSA Annual Meeting, Frontiers in Optics, Tuscon, Arizona, October 18, 2005 (**Invited)**
44. Y. Fainman, K. Tetz, U. Levy, W. Nakagawa, C.-H. Tsai, C.-H. Chen, L. Pang, M. Nezhad, M. Abashin, A. Nesci, and P. C. Sun, "Nanophotonics for Information Systems Integration" presented at the IEEE/LEOS Annual Meeting, Sydney, Australia, October 23-28, 2005 **(Invited)**
45. Yeshaiahu Fainman, Kevin A. Tetz, Rostislav Rokitski, and Maziar Nezhad, "Characterization of ultra short surface plasmon polaritons in nanohole arrays," presented at the18-th IEEE/LEOS Annual Meeting, October 23-28, Sydney, Australia 2005(**Invited)**
46. Y. Fainman, K. Tetz, U. Levy, W. Nakagawa, C.-H. Tsai, C.-H. Chen, L. Pang, M. Nezhad, M. Abashin, A. Nesci, and P. C. Sun, "Nanophotonics for Information Systems Integration" presented at the 18-th IEEE/LEOS Annual Meeting, October 23-28, Sydney, Australia 2005(**Invited)**

During Period 2005-2006

47. L. J. Sham, Plenary talk, "Restoring coherence lost", Symposium on the Physics of Quantum Electronics, Snowbird, Utah, January 3-6, 2006.
48. L. J. Sham, Invited talk, "Electron spin decoherence by nuclear spins", Conference on "Quantum computing and Many-Body Systems", Key West, Florida, January 31 – February 3, 2006.
49. L. J. Sham, Invited talk, "Resotring lost coherence", PITP/CQIQC Workshop on Decoherence, Vancouver, Canada, February 20-22, 2006.
50. L. J. Sham, Invited talk, "Optical control of electron spins in quantum dots for quantum computation", International Workshop on Solid-State Quantum Computing, Nanjing, China, June 8-12, 2006.
51. Wang Yao, Ren-Bao Liu, and L. J. Sham, Invited talk, "Optically manipulating spins in semiconductor quantum dots", 28th International Conference on the Physics of Semiconductors, Vienna, Austria, July 24-28, 2006. Conference Proceedings: J. Applied Phys., in press.

52. C.W. Tu, S. Suraprapapich, Y.M. Shen, Y. Fainman, S. Panyakeow, "Growth of Self-Assembled Quantum Dots, Quantum Rings, and Lateral Bi-Quantum-Dot Molecules by Gas-Source Molecular Beam Epitaxy", Proc. State-of-the-Art Program on Compound Semiconductors 45, Electrochemical Society (2006).
53. C.W. Tu, S. Suraprapapich, Y.M. Shen, Y. Fainman, S. Panyakeow, "Growth of Self-Assembled Quantum Dots, Quantum Rings, and Lateral Bi-Quantum-Dot Molecules by Gas-Source Molecular Beam Epitaxy", State-of-the-Art Program on Compound Semiconductors 45 (SOTAPOCS 45), Cancun, Mexico, 29 Oct. – 3 Nov. 2006.
54. S. Suraprapapich, Y.M. Shen, Y. Fainman, S. Panyakeow, and C.W. Tu, "Self-Assembled Quantum Dots, Quantum Rings, and Lateral Bi-Quantum-Dot Molecules Grown by Gas-Source Molecular Beam Epitaxy", North America MBE Conference, Duke University, Durham, NC, 8-11 October 2006.
55. S. Suraprapapich, Y.M. Shen, V.A. Odnoblyudov, Y. Fainman, S. Panyakeow, and C.W. Tu, "Self-Assembled Lateral Bi-Quantum-Dot Molecule Formation by Gas-Source Molecular Beam Epitaxy", International Conference on Molecular Beam Epitaxy, Waseda University, Tokyo, Japan, 3-8 September 2006.
56. S. Suraprapapich, Y.M. Shen, Y. Fainman, S. Panyakeow, and C.W. Tu, "Growth and Characterization of Self-Assembled Lateral Bi-Quantum-Dot Molecules", International Symposium on Compound Semiconductors, University of British Columbia, Vancouver, Canada, 13-17 August 2006.
57. S. Suraprapapich, Y.M. Shen, Y. Fainman, S. Panyakeow, and C.W. Tu, "The Effects of Rapid Thermal Annealing on Lateral Bi-Quantum-Dot Molecules Grown by Gas-Source Molecular Beam Epitaxy", 48th Electronic Materials Conference, Pennsylvania State University, University Park, PA, 28 June – 30 June 2006.
58. Y. Fainman, " Nanophotonics for Information systems integration, Photonics West, SPIE, January, 2006 **(Invited)**
59. Y. Fainman, " Nanophotonics for information systems integration, OSA Topical Meeting, April 26-28, Mohegan Sun, CT, 2006 **(Invited)**
60. Y. Fainman, " Ultrafast Informnation Processing, XII Conference on Laser Optics, St. Petersburg, Russia, June 26-30, 2006**(Invited)**
61. Y. Fainman "Information Processing with Ultrashort Laser Pulses, 5-th Intl. Workshop on Information Optics, Toledo, Spain, June 5-7, 2006 **(Invited)**
62. Y. Fainman, "Optoifluidics for adaptive optics and sensing applications, IEEE/LEOS Topical Meeting on Optoifluidics, Quebeck City, July 17-19, 2006 **(Invited)**
63. Y. Fainman "Nanophotonic structures and devices with polymers," 232-nd ACS National Meeting, San Francisco, CA Sept. 110-14, 2006 **(Invited)**
64. K. Tetz, M. Nezhad, L. Pang, Y. Fainman, "Optofluidic Plasmonics," SPIE annual meeting, San Diego, August, 2006
65. Y. Fainman, U. Levy, A. Groisman, K. Kampbell, S. Mookherjea, K. Tets, R. Rokitski, M. Nezhad, and L. Pang, "Optofluidics for Adaptation and Sensing" OSA Annual Meeting, October 10, 2006 Rochester, NY 2006 **(Invited)**

b. Consultative and advisory functions

1. "Quantum device technologies – applying 2-D photonic crystals," DARPA QuIST PIs Review Conference, November 16-19, 2004, Scotsdasle, Arizona

During Period 2004-2005:

2. Y. Fainman, General Chair and Program co-Chair of the first OSA Topical Meeting on Nanophotonics for Optical Information Systems Integration," San Diego, April 14-16, 2005
3. Y. Fainman, "Optofluidics for Adaptive and Nonlinear Optics" Optofluidics Center, DARPA's Opto-Electronic Centers Review, Sonoma County, Summer 2005
4. "Quantum device technologies – applying 2-D photonic crystals," AFOSR PIs Review Conference, October 7, 2005, Chicago, Illinois
5. Y. Fainman, Chairs of the subcommittee on "Optical Interconnects and Signal Processing," IEEE/LEOS Annual Meeting, Sydney, October 23-28, 2005

During Period 2005-2006:

6. Y. Fainman"A Unified view on Nanophotonics," MITRE Nanophotonics Workshop, February 14-15, Washington, DC, 2006 (**Invited**)
7. Y. Fainman, "Optofluidics for Adaptive and Nonlinear Optics" Optofluidics Center, DARPA's Opto-Electronic Centers Review, Utah, Summer 2006
8. Y. Fainman, "Nanophotonics for optical delay engineering," NSF Grantees Conference, Taskegee Univ, AL, June 13-15, 2006
9. Y. Fainman, Chairs of the subcommittee on "Optical Interconnects and Signal Processing," IEEE/LEOS Annual Meeting, Sydney, October, 2006
10. Y. Fainman " Interconnection technology foir intrachip communications, DARPA Intra-chip communications workshop, March 27-28, 2006, Arlington, VA
11. Y. Fainman " Optofluidics for adaptive optics and sensing", DARPA Center on Optofluidics Integration, Retreat, Harvard University, April 2006.
12. Y. Fainman, "Processing information with Femtosecond pulses," DARPA AOSP Program Review, San Francisco, August 7-10, 2006
13. Y. Fainman, "Nanophoitonics and Optofluidics, " Sandia National Laboratory, September 7, 2006
14. Y. Fainman, "Optofluidics for adaptation and sensing," DARPA Optocenters Review, July 9-12, 2006
15. Y. Fainman "Optical feedback with gain processing," DARPA P3A Workshop, August 22, 2006, DC

7. New discoveries: None

8. Honors/Awards: None
C.W. Tu was elected Fellow of the AVS, 2004
Y. Fainman was elected Fellow of the SPIE, 2004.